**Instituto de Física Teórica**
**Universidade Estadual Paulista**

MASTERS DISSERTATION IFT–D.001/16

# Structure of weakly-bound three-body systems in two dimension

John Hadder Sandoval Quesada

Advisor

Dr. Marcelo Takeshi Yamashita

March 21, 2016

# Acknowledgment

A thesis is not a solitary project, where the author is the only one concerned on it. Instead, it is the sum of many hours of hard work of countless people supporting and guiding the author with the purpose that each minute spent on him, contribute to give wisdom in all possible roads of life. For those people, my sincere gratitude.

Firstly, I would like to express my gratefulness to my advisor Prof. Marcelo Takeshi Yamashita. He has been a continuous support in my studies and related research, for his patience, motivation, and immense knowledge. His guidance helped me in all the time of research and writing of this thesis. I could not have imagined having a better advisor and mentor.

Since I arrived to the Institute of theoretical physics I have met too many wise physicists who have been helped me through this journey

Prof. Aksel S. Jensen (AU/Denmark), which help us to analyze in many different ways the results. Thanks too for encourage and support me in the application of the Aarhus University.

Dr. Filipe Furlan Bellotti, who guide and give me values advice for the thesis.

Dr. Nikolaj Zinner, who will be my main supervisor in Aarhus University.

My colleagues and friends from the IFT, F. Serna, S. Parra, C. Guitiérrez, J. Rivera and D. Santos. Who give me physics discussions and fun moments.

My family whom I miss every day. My mother Magali Quesada, my father José Sandoval, my sisters Heidy Sandoval and Maricely Sandoval, my nieces and nephews, Silvia Carolina, Paula Andrea, David Santiago, Juan Sebastián and Mateo.

Foundation CAPES (Coordenação de Aperfeiçoamento de Pessoal de Nível Superior) of the Ministry of Education in Brazil.

To the Institute of theoretical physics (IFT/UNESP).

*"The more I try understand the universe,*
*the more magical and complex it becomes."*

John H. Sandoval.

# Resumo

Este trabalho foca no estudo de sistemas de poucos corpos em duas dimensões no regime universal, onde as propriedades do sistema quântico independem dos detalhes da interação de curto alcance entre as partículas (o comprimento de espalhamento de dois corpos é muito maior que o alcance do potencial). Nós utilizamos a decomposção de Faddeev para escrever as equações para os estados ligados. Através da solução numérica dessas equações nós calculamos as energias de ligação e os raios quadráticos médios de um sistema composto por dois bósons (A) e uma partícula diferente (B). Para uma razão de massas $m_B/m_A = 0.01$ o sistema apresenta oito estados ligados de três corpos, os quais desaparecem um por um conforme aumentamos a razão de massas restando somente os estados fundamental e primeiro excitado. Os comportamentos das energias e dos raios para razões de massa pequenas podem ser entendidos através de um potencial do tipo Coulomb a curtas distâncias (onde o estado fundamental está localizado) que aparece quando utilizamos uma aproximação de Born-Oppenheimer. Para grandes razões de massa os dois estados ligados restantes são consistentes com uma estrutura de três corpos mais simétrica. Nós encontramos que no limiar da razão de massas em que os estados desaparecem os raios divergem linearmente com as energias de três corpos escritas em relação ao limiar de dois corpos.

**Palavras Chaves**: Estados Efimov; Distribuição de momento; Problema de poucos corpos;

**Áreas do conhecimento**: Física teórica; Física atômica, Física de poucos corpos

# Abstract

This work is focused in the study of two dimensional few-body physics in the universal regime, where the properties of the quantum system are independent on the details of the short-range interaction between particles (the two-body scattering length is much larger than the range of the potential). We used the Faddeev decomposition to write the bound-state equations and we calculated the three-body binding energies and root-mean-square (rms) radii for a three-body system in two dimensions compounded by two identical bosons (A) and a different particle (B). For mass ratio $m_B/m_A = 0.01$ the system displays eight three-body bound states, which disappear one by one as the mass ratio is increased leaving only the ground and the first excited states. Energies and radii of the states for small mass ratios can be understood quantitatively through the Coulomb-like Born-Oppenheimer potential at small distances where the lowest-lying of these states are located. For large mass ratio the radii of the two remaining bound states are consistent with a more symmetric three-body structure. We found that the radii diverge linearly at the mass ratio threshold where the three-body excited states disappear. The divergences are linear in the inverse energy deviations from the corresponding two-body thresholds.

**Keywords**: Efimov states; Momentum distribution; Few-body problem;

**Areas of knowledge**: Theoretical Physics; Atomic Physics, Few-body physics

# Table of Contents

# List of Figures

# List of Tables

# Chapter 1

# Introduction

Recently, the study of few-body correlations has received a special attention due to the possibility of changing the two-body interactions inside ultracold atomic traps by using Feshbach resonance techniques[1]. The experimental realization of such traps also allows the construction of a quasi two-dimensional (2D) environment[2, 3] where, in many situations, the physics involved differs considerably from the three-dimensional (3D) case [4, 5]. In the case of diluted atomic gases compounded by neutral atoms the interactions between them are of very short-range compared to the two-body scattering length [6, 7, 8]. This implies that the (low-energy) observables are universal: they do not depend on the details of the interaction [9, 10]. In order to study this universal regime we may consider a zero-range interaction.

The universal regime can be described by only few scale-parameters [11]. Furthermore, in a three-boson system the number of these scales is drastically affected by the dimensionality of the system. In 3D, we need both a two- and a three-body scale to describe the observables [12]. In contrast in 2D all observables can be expressed as functions of only one two-body scale parameter, e.g. the two-body scattering length [9, 10]. This difference is closely related to the appearance of the Efimov effect [13] in 3D and its absence in 2D [14, 17]. The extra scale appearing in 3D may be explained by the emergence of the Thomas collapse.

We already have an extensive amount of investigations about the energy spectrum of three-atoms in 2D [15, 16, 17, 18, 19, 20, 21, 22], but very little information can be found in the literature about the three-body structures [9]. For three identical bosons we have only two three-body bound states with energies ($E_3$) proportional to the two-body energy ($E_2$) and given by $E_3 = 16.52E_2$ and $E_3 = 1.27E_2$, respectively for the ground and excited states [15]. However, considering an asymmetric systems as AAB formed by two identical bosons and a distinguishable particle we can increase the number of three-body bound states only by changing the mass asymmetry [19]. When the mass ratio, $m_B/m_A$, between particles B and A is decreased, then B may be easier exchanged between the identical A-particles, which in turn generates an effective potential with infinite attraction in the limit of $m_B/m_A \to 0$ [20, 22, 24]. This provides a prescription for an arbitrary increase of the number of three-body bound states.

An interesting question is how the three-body bound-state structure varies close to the mass threshold where the state disappear into the continuum. In general, the structure variation with the mass ratio is not known in 2D for neither ground or excited states. If the quantum mechanical wave function is known it is in principle very direct to study the calculated density distribution. However, this may be too elaborate for a first overall orientation. The simplest observable quantities that carry structure information are the relative average distances between pairs of particles. Here the second moment is most often used as the measure, but obviously only as a constraint on the possible structure. First order or higher moments would clearly add information to the spatial distribution.

The thesis work is organized as follows. In chapter 2 we set and study in details the formalism used in a collision process. We obtain expression for the transition operator for two-body and three-body system in two dimensions for a local and separable interaction such as a Dirac-$\delta$ potential. By using the Faddeev method, we obtain the Faddeev equations for a three-body system where we use them to obtain an expression for a three-body bound state equation in two dimensions. In chapter 3 by using concepts of quantum mechanics, we obtain expressions for mean square radius in momentum space for a three-body system compound by three distinguishable particles ABC. In chapter 4 we provide an algorithm to solve the mean square radii equations obtained in chapter 3. Finally in chapter 5 we present our summary, conclusions and perspectives.

# Chapter 2

# Formalism: Three-body dynamics

In this chapter we shall first define the transition operator, usually called as transition matrix, $T$, or only $T$-matrix. Because $T$-Matrix is related with the Green function we study it in details. Once defined the $T$-Matrix, we calculate it, for two-body and three-body system with short-range interaction such as the Dirac-$\delta$ potential. We will follow closely the theorical development presented in Charles. J. Joachain [38].

Next we discuss the Lipppmann-Schwinger equation's problems for three or more -body systems and the solution given by L. D. Faddeev [26]. This analysis leads to the Faddeev equations for three-body problems. Also we calculate those Faddeev equations for two-dimensional case and the matrix elements in a bound state context.

By extracting the $k$-component of the transition operator in a bound state context for the Faddeev equations in two-dimensions, we define the set of coupled spectator functions by projecting this $k$-component in a momentum space basis known as the Jacobi relative momentum coordinate between particles. Finally, combining the spectator functions and the Green function we get the wave function for a three-body bound state.

## 2.1 $T$-Matrix

The operator is defined by the relation

$$T(E) \equiv V + VG^{(\pm)}V = V + V \lim_{\epsilon \to 0^+} \frac{1}{E - H \pm i\epsilon} V \tag{2.1}$$

where $V$ is the full interaction between all the particles and $G^{(\pm)} = \lim_{\epsilon \to 0^+} \frac{1}{E-H \pm i\epsilon}$ is the Green's operator. In order to have a good understanding of this equation we may study in details the Green Operator.

### 2.1.1 The Green's Function

#### Free Green's Function

Considering a time-independent Schrödinger equation that describes a system of two colliding particles interacting by a potential $U(\vec{r})$ which depends only on their relative coordinates $\vec{r}$

$$[\nabla^2_{\vec{r}} + k^2]\psi(k,\vec{r}) = U(\vec{r})\psi(k,\vec{r}), \tag{2.2}$$

where $\psi(k,\vec{r})$ is a solution that satisfy equation (2.2) which involves an incoming plane wave and a scattered wave, $k$ is the wave vector. Also the right-hand side from equation (2.2) is known as an inhomogeneous term that without it, we get the homogenous Schrödinger equation $[\nabla^2_{\vec{r}}+k^2]\phi(k,\vec{r}) = 0$. The general solution $\psi(k,\vec{r})$ is written as

$$\psi(k,\vec{r}) = \phi(k,\vec{r}) + \int d\vec{r'} G_0(k,\vec{r},\vec{r'})U(\vec{r'})\psi(k,\vec{r'}) \tag{2.3}$$

where $\phi(k,\vec{r})$ is a solution of the homogeneous Schrödinger equation. The Green's function corresponding to the $\nabla^2_{\vec{r}}$ and the number $k^2$ follow the next relation

$$[\nabla^2_{\vec{r}} + k^2]G_0(k,\vec{r},\vec{r'}) = \delta(\vec{r}-\vec{r'}). \tag{2.4}$$

We want to determine the free Green's function $G_0(\vec{r},\vec{r}\,')$. It is convenient for that purpose to work in wave vector space.

We are going to write the green's function as

$$G_0(\vec{r},\vec{r}\,') = (2\pi)^{-3}\int g_0(\vec{k'},\vec{r'})\exp{(i\vec{k'}.\vec{r})}d\vec{k'} \tag{2.5}$$

where $g_0(\vec{k'},\vec{r'})$ represent just an auxiliary function which will help to do the calculations. Replacing it into equation (2.4) we get

$$(2\pi)^{-3}[\nabla^2_{\vec{r}} + k^2]\int g_0(\vec{k'},\vec{r'})\exp{(i\vec{k'}.\vec{r})}d\vec{k'} = \delta(\vec{r}-\vec{r'}), \tag{2.6}$$

using the integral representation for the delta function

$$\delta(\vec{r}-\vec{r'}) = (2\pi)^{-3}\int \exp\{i\vec{k'}.(\vec{r}-\vec{r'})\}d\vec{k'} \tag{2.7}$$

we obtain for $g_0(\vec{k'},\vec{r'})$

$$g_0(\vec{k'},\vec{r'}) = \frac{\exp{(-i\vec{k'}.\vec{r'})}}{k^2-k'^2} \tag{2.8}$$

and therefore our equation (2.5) becomes

$$G_0(\vec{r},\vec{r}\,') = -(2\pi)^{-3}\int \frac{\exp{\{i\vec{k'}.(\vec{r}-\vec{r'})\}}}{k'^2-k^2}d\vec{k'} \tag{2.9}$$

As we can see the equation (2.9) has poles at $k' = \pm k$, due to that we need to avoid these singularities and give a meaning to the integral. In order to do this, we use the boundary condition that assume the potential $V(\vec{r})$ tends to zero faster than $r^{-1}$ as $r \to \infty$, in other words, the stationary scattering wave function will have an asymptotic behavior, that lead us to an outgoing spherical wave. Due to that we will denote by $G_0^+(\vec{r}, \vec{r}')$ and $\psi_{\vec{k}_i}^+(\vec{r})$ the corresponding free Green's function and the stationary outgoing scattering wave respectively. As we saw from equation (2.1) our Green function possess two different signs that are totally relates which pole we will choose and depending on the pole chosen the behavior of our scattered wave (incoming or outgoing wave). We set $\vec{r} - \vec{r}' \equiv \vec{R}$, and chose polar coordinates in a way that the $z$ axis coincides with the vector $\vec{R}$ as we can see in Figure (2.1)

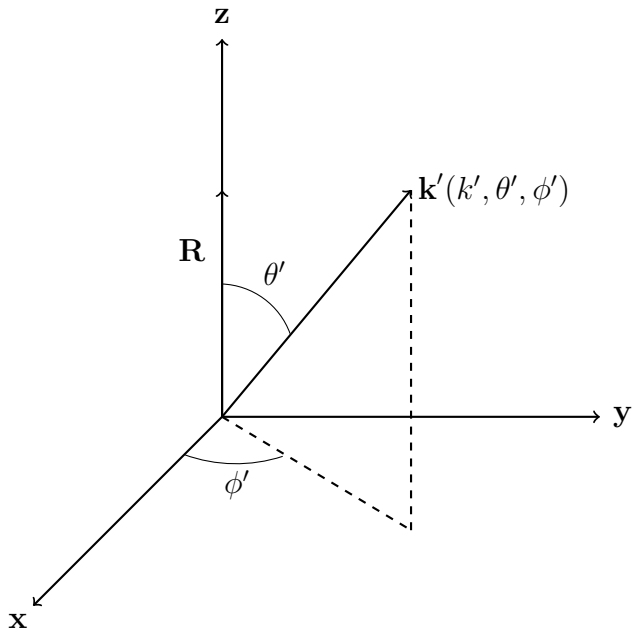


Figura 2.1: Illustration of the vectors $\vec{R}$ and $\vec{k}'$ of the text.

the equation (2.9) then is

$$G_0(R) = -(2\pi)^{-3} \int_0^\infty dk' k'^2 \int_0^\pi d\theta' \sin(\theta') \int_0^{2\pi} d\phi' \frac{\exp\{ik' R \cos\theta'\}}{k'^2 - k^2}, \tag{2.10}$$

performing the angular integrations, we get

$$G_0(R) = -(4\pi^2 R)^{-1} \int_{-\infty}^{\infty} \frac{k' \sin(k'R)}{k'^2 - k^2} dk' \tag{2.11}$$

here we used the fact that the integrand is an even function of $k'$ to extend the integral on the $k'$ from $-\infty$ to $\infty$. We may use the next relations

$$\frac{k'}{k'^2 - k^2} = \quad \tfrac{1}{2}\left[\tfrac{1}{k'-k} + \tfrac{1}{k'+k}\right] \tag{2.12}$$

$$\sin(k'R) = \quad \tfrac{1}{2i}\left(e^{(ik'R)} - e^{(-ik'R)}\right) \tag{2.13}$$

we may also write

$$G_0(R) = (16\pi^2 iR)^{-1}\left\{\int_{-\infty}^{\infty} e^{(ik'R)}\left[\frac{1}{k'-k} + \frac{1}{k'+k}\right]dk' - \int_{-\infty}^{\infty} e^{(-ik'R)}\left[\frac{1}{k'-k} + \frac{1}{k'+k}\right]dk'\right\}. \tag{2.14}$$

Those integrals can be analyzed in the complex $k'-plane$ and be solved by using Cauchy's theorem,

$$I_1 \equiv \oint_{C_1} dk' e^{ik'R}\left[\frac{1}{k'+k} + \frac{1}{k'-k}\right], \tag{2.15}$$

$$I_2 \equiv \oint_{C_2} dk' e^{-ik'R}\left[\frac{1}{k'+k} + \frac{1}{k'-k}\right] \tag{2.16}$$

the integral must contain closed paths. For the integral $I_1$ the path $C_1$ is a semi-circle in the counterclockwise direction in the semi-plane where, $Im\,k' > 0$. Otherwise the integral $I_2$ have a semi-circle path $C_2$, closed in the clockwise direction in the semi-plane where, $Im\,k' < 0$. Those semi-circles are larger, so that the contribution to the integral tends to zero as we let the radius of $C_1$ and $C_2$ tend to infinity. The integrals (2.15 and 2.16) is then equal to its value along the real axis, for which we have four possible choices of paths $\mathbf{P}_1$, $\mathbf{P}_2$, $\mathbf{P}_3$, $\mathbf{P}_4$, as shown in figure (2.2).

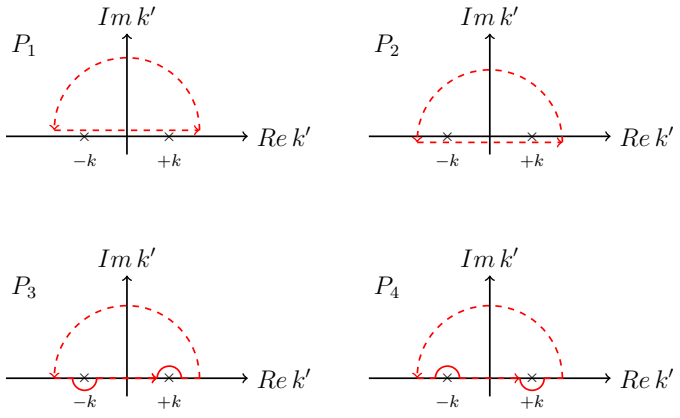


Figura 2.2: The four possible integration contours for the evaluation of the integral $I_1$.

Applying Cauchy's theorem, we then obtain for the integral $I_1$ the values showed in Table (2.1)

| Path | $C_1$ | $I_1$ |
|---|---|---|
| P1 | 0 | 0 |
| P2 | poles $\pm k$ | $2\pi i\left(e^{ikR}+e^{-ikR}\right)$ |
| P3 | pole $-k$ | $2\pi i e^{-ikR}$ |
| P4 | pole $+k$ | $2\pi i e^{ikR}$ |

Table 2.1: Result for the integral $I_1$ respect to the inclusion of the poles $\pm k$ inside the path $C_1$ closed by a semicircle in counterclockwise direction.

proceeding in the same way with the second integral, just knowing that the contour are closed now in the lower-half $k'$ plane, we find the next values for the contribution of this integral showed in Table (2.2)

| Path | $C_2$ | $I_2$ |
|---|---|---|
| P1 | poles $\pm k$ | $-2\pi i\left(e^{ikR}+e^{-ikR}\right)$ |
| P2 | 0 | 0 |
| P3 | pole $+k$ | $-2\pi i e^{-ikR}$ |
| P4 | pole $-k$ | $-2\pi i e^{ikR}$ |

Table 2.2: Result for the integral $I_2$ respect to the inclusion of the poles $\pm k$ inside the path $C_2$ closed by a semicircle in clockwise direction.

Therefore we conclude that there is only one way of defining the Green's function $G_0^+(R)$ in such a way that it behaves as a purely outgoing wave for large values of r or of R. That is through the path $\mathbf{P}_4$

$$\begin{aligned} G_0^+(R) &= (4\pi^2 R)^{-1}\oint_{p_4}\frac{k'\sin(k'R)}{k'^2-k^2}dk' \\ &= -(16\pi^2 R)^{-1}\left[2\pi i e^{ikR}-(-2\pi i e^{ikR})\right] \\ &= -(4\pi R)^{-1}e^{ikR} \\ &= -\frac{1}{4\pi}\frac{e^{ikR}}{R} \end{aligned} \tag{2.17}$$

or returning to the original variables $\vec{r}$ and $\vec{r'}$

$$G_0^+(\vec{r},\vec{r'}) = -\frac{1}{4\pi}\frac{e^{ik|\vec{r}-\vec{r'}|}}{|\vec{r}-\vec{r'}|} \tag{2.18}$$

This is the free Green's function for an outgoing spherical wave.

**Total Green's Function**

Going back to the definition of the transition operator $T(E) \equiv V + VG^{(\pm)}V$, it is defined in terms of the total Green function, then we are going to find the relation between the already found free Green function $G_0^{(\pm)}(\vec{r}, \vec{r'})$ and the total Green function $G^{(\pm)}(\vec{r}, \vec{r'})$.

From the Lippman-Schwinger equation expressed as

$$\psi_{k_i}^{+}(\vec{r}) = \phi_{k_i}(\vec{r}) + \psi_{sc}^{+}(\vec{r}), \tag{2.19}$$

where $\phi_{k_i}(\vec{r})$ represent the solution of the homogenous Schrödinger equation mentioned before and $\psi_{sc}^{+}(\vec{r})$ represent the scattered outgoing wave, and must satisfy the inhomogeneous equation

$$[\nabla_r^2 + k^2 - U(\vec{r})]\psi_{sc}^{+}(\vec{r}) = U(\vec{r})\phi_{k_i}(\vec{r}). \tag{2.20}$$

Now, supposing that we know the total Green's function of the problem $G^{+}(\vec{r}, \vec{r'})$, and it have to satisfy

$$[\nabla_r^2 + k^2 - U(\vec{r})]G^{+}(\vec{r}, \vec{r'}) = \delta(\vec{r} - \vec{r'}) \tag{2.21}$$

and such that comparing with equation (2.3), but in a general case, knowing the total Green function

$$\psi_{sc}^{+}(\vec{r}) = \int G^{+}(\vec{r}, \vec{r'})U(\vec{r'})\phi_{k_i}(\vec{r})d\vec{r'}. \tag{2.22}$$

Now we determine the total Green's function by replacing (2.4) into the equation (2.21).

$$\begin{aligned} [\nabla_r^2 + k^2]G^{+}(\vec{r}, \vec{r'}) &= \delta(\vec{r} - \vec{r'}) + U(\vec{r})G^{+}(\vec{r}, \vec{r'}) \\ &= [\nabla_r^2 + k^2]G_0(\vec{r}, \vec{r'}) + U(\vec{r})G^{+}(\vec{r}, \vec{r'}). \end{aligned} \tag{2.23}$$

Let us now consider some properties of the $\delta$-function to rewrite $U(\vec{r})G^{+}(\vec{r}, \vec{r'})$ in an integral form. Using equation (2.4) and replacing $[\nabla_r^2 + k^2] \equiv \mathcal{L}(r)$ (which is a linear operator) we get

$$\begin{aligned} [\nabla_r^2 + k^2]G^{+}(\vec{r}, \vec{r'}) &= [\nabla_r^2 + k^2]G_0(\vec{r}, \vec{r'}) + \int \delta(\vec{r} - \vec{r''})U(\vec{r''})G^{+}(\vec{r''}, \vec{r'})d\vec{r''} \\ &= [\nabla_r^2 + k^2]G_0(\vec{r}, \vec{r'}) + \int [\nabla_r^2 + k^2]G_0(\vec{r}, \vec{r''})U(\vec{r''})G^{+}(\vec{r''}, \vec{r'})d\vec{r''} \end{aligned} \tag{2.24}$$

and therefore

$$\begin{aligned} \mathcal{L}G^{+}(\vec{r}, \vec{r'}) &= \mathcal{L}G_0(\vec{r}, \vec{r'}) + \textstyle\int \mathcal{L}G_0(\vec{r}, \vec{r''})U(\vec{r''})G^{+}(\vec{r''}, \vec{r'})d\vec{r''} \\ \mathcal{L}G^{+}(\vec{r}, \vec{r'}) &= \mathcal{L}\left[G_0(\vec{r}, \vec{r'}) + \textstyle\int G_0(\vec{r}, \vec{r''})U(\vec{r''})G^{+}(\vec{r''}, \vec{r'})d\vec{r''}\right] \end{aligned} \tag{2.25}$$

finally we obtain for the total Green's function as an integral equation

$$G^+(\vec{r},\vec{r'}) = G_0(\vec{r},\vec{r'}) + \int G_0(\vec{r},\vec{r''})U(\vec{r''})G^+(\vec{r''},\vec{r'})d\vec{r''}. \tag{2.26}$$

or

$$G^+ = G_0^+ + G_0^+ U G^+. \tag{2.27}$$

### 2.1.2 Relation with Collision Operator, Second form Dirac notation and Matrix elements of the Transition Operator

In the scattering theory, the collision operator, $S$, and the transition operator, $T$, are two important operators which are related with the observables measured from collision experiments. Therefore the importance of studing their relation. If we denote by $\phi$, the asymptotic free state vectors, that satisfy the Schrödinger equation of a free particle, $H_0\phi = E\phi$, we may find the matrix elements of the $T$-matrix which are given by $\langle\Phi_\beta|T|\Phi_\alpha\rangle$, where $\Phi_\beta$ and $\Phi_\alpha$ are asymptotic states with energies $E_\beta$ and $E_\alpha$ respectively. And those elements connect with the $S$-matrix by the next relation (details of the $S$-matrix are given in Appendix A)

$$\langle\Phi_\beta|S|\Phi_\alpha\rangle = \delta_{\alpha\beta} - 2\pi i\delta(E_\beta - E_\alpha)\langle\Phi_\beta|T|\Phi_\alpha\rangle \tag{2.28}$$

indeed, for $E_\alpha \neq E_\beta$ the second term on the right-hand side of equation (2.28) vanish independently of the value of the matrix elements $\langle\Phi_\beta|T|\Phi_\alpha\rangle$. On the contrary, for $E_\alpha = E_\beta$, the second term on the right-hand side of equation (2.28), constitute the non-trivial part of the $S$-matrix, the fact that $i\delta(E_\beta - E_\alpha)$ is actually infinite, is not a problem since we eventually consider transition into a group of states in the continuum centered $E = E_\alpha = E_\beta$, in other words the delta function ensures energy conservation in a transition $\Phi_\alpha \to \Phi_\beta$.

Writing the transition operator as:

$$T = V + VG_0^{(\pm)}T = V + TG_0^{(\pm)}V, \tag{2.29}$$

*

*which can be demonstrated that this relation is equivalent with equation (2.1) by self-iteration and using the relation (2.27) as

$$\begin{aligned} T = &\quad V + VG_0^{(\pm)}\left(V + VG_0^{(\pm)}\left(V + VG_0^{(\pm)}...\right)\right) \\ = &\quad V + V\left(G_0^{(\pm)} + G_0^{(\pm)}VG_0^{(\pm)} + ...\right)V \\ = &\quad V + VG^{(\pm)}V. \end{aligned} \tag{2.30}$$

The matrix elements in a momentum spaces basis of the transition operator are possible to find by using equation (2.29), since we know the form of the free Green operator and how it acts in a momentum space state. Those elements will be useful since they becomes in an integral equation, which can be used later in the computation of the spectator functions. Then, the matrix elements of the transition operator from a transition between the state $|\vec{p'}\rangle$ to a state $|\vec{p}\rangle$ could be rewritten as an integral equation as

$$\begin{aligned}
\langle\vec{p}|T|\vec{p}'\rangle &= \langle\vec{p}|V|\vec{p}'\rangle + \langle\vec{p}|V\frac{1}{E-H_0\pm i\epsilon}T|\vec{p}'\rangle,\\
\langle\vec{p}|T|\vec{p}'\rangle &= \langle\vec{p}|V|\vec{p}'\rangle + \langle\vec{p}|V\frac{1}{E-H_0\pm i\epsilon}\int d^3p''|\vec{p}''\rangle\langle\vec{p}''|T|\vec{p}'\rangle,\\
\langle\vec{p}|T|\vec{p}'\rangle &= \langle\vec{p}|V|\vec{p}'\rangle + \int d^3p''\langle\vec{p}|V\frac{1}{E-H_0\pm i\epsilon}|\vec{p}''\rangle\langle\vec{p}''|T|\vec{p}'\rangle,\\
\langle\vec{p}|T|\vec{p}'\rangle &= \langle\vec{p}|V|\vec{p}'\rangle + \int d^3p''\langle\vec{p}|V|\vec{p}''\rangle\frac{1}{E-\frac{p''^2}{2m}\pm i\epsilon}\langle\vec{p}''|T|\vec{p}'\rangle. \qquad (2.31)
\end{aligned}$$

from the collision experiments we get measurable data for the cross-section, then through this way we may connect the experiments with the scattering theory. The collision operator describes the connection between the initial and final states of the system and it is highly related with the transition operator as we see in equation (2.28). From the scattering theory we have a relation between the transition operator and the scattering amplitude given by $f = |T|$ where $f$ is the scattering amplitude, and at the same time the scattering amplitude lead us to a differential cross section $\frac{d\sigma}{d\Omega} = |f|^2$, where $\sigma$ is the cross-section, which we use to compare with the collision experiments.

In three-dimensional systems the study of phase-shift and cross-section by the scattering theory it is widely done in several text books. In two-dimensional problems there are some subtle details. A good description can be found in [27, 28].

## 2.2 Two-body T-Matrix for Dirac-$\delta$ potential

We determine the T-Matrix for a two-body system, considering a zero-range potential. The Dirac-$\delta$ potential is also separable and may be written in the operator form as

$$V = \lambda|\chi\rangle\langle\chi|, \qquad (2.32)$$

where $\lambda$ is the potential strength.
Then using the transition matrix, equation (2.29) and replacing the above potential we get

$$T(E) = V + VG_0(E)T(E),$$

$$T(E) = \lambda|\chi\rangle\langle\chi| + \lambda|\chi\rangle\langle\chi|G_0(E)T(E), \qquad (2.33)$$

multiplying by $\langle\chi|G_0(E)$ the last expression, and solving for $\langle\chi|G_0(E)T(E)$ we obtain

$$\langle\chi|G_0(E)T(E) = \lambda\langle\chi|G_0(E)|\chi\rangle\langle\chi| + \lambda\langle\chi|G_0(E)|\chi\rangle\langle\chi|G_0(E)T(E),$$

$$(1 - \lambda\langle\chi|G_0(E)|\chi\rangle)\langle\chi|G_0(E)T(E) = \lambda\langle\chi|G_0(E)|\chi\rangle\langle\chi|,$$

$$\langle\chi|G_0(E)T(E) = \frac{\lambda\langle\chi|G_0(E)|\chi\rangle\langle\chi|}{1 - \lambda\langle\chi|G_0(E)|\chi\rangle}. \tag{2.34}$$

we note that this term in equation (2.34) appears in equation (2.33), then if we replace this term that leads to

$$T(E) = \lambda|\chi\rangle\langle\chi| + \frac{\lambda^2|\chi\rangle\langle\chi|G_0(E)|\chi\rangle\langle\chi|}{1 - \lambda\langle\chi|G_0(E)|\chi\rangle},$$

$$T(E) = \lambda|\chi\rangle\left(1 + \frac{\lambda\langle\chi|G_0(E)|\chi\rangle}{1 - \lambda\langle\chi|G_0(E)|\chi\rangle}\right)\langle\chi|, \tag{2.35}$$

which in compact form becomes

$$T(E) = |\chi\rangle\tau(E)\langle\chi|, \tag{2.36}$$

the matrix elements of $\tau(E)$ are given by

$$\tau(E) = \left(\lambda^{-1} - \langle\chi|G_0(E)|\chi\rangle\right)^{-1}. \tag{2.37}$$

Introducing the identity $\hat{1} = \int d^Dp|\vec{p}\rangle\langle\vec{p}|$ in equation (2.37), we may write the integral form of this T-matrix

$$\begin{aligned}\tau(E) &= \left(\lambda^{-1} - \int\int d^Dp'd^Dp\langle\chi|\vec{p'}\rangle\langle\vec{p'}|G_0(E)|\vec{p}\rangle\langle\vec{p}|\chi\rangle\right)^{-1} \\ &= \left(\lambda^{-1} - \int d^Dp\frac{g(p)^2}{E - \frac{p^2}{2m_{red}} + i\epsilon}\right)^{-1}\end{aligned} \tag{2.38}$$

here $m_{red}$ is the two-body reduced mass and $g(p) \equiv \langle\vec{p}|\chi\rangle$ is the form factor of the potential $V$. The form factor have spherical symmetry and in the Dirac-$\delta$ potential $g(p) = \langle\vec{p}|\chi\rangle = \langle\chi|\vec{p}\rangle = 1$, which is demonstrated below.

Calling by $\vec{R}$ as a vector that links two particles, we may calculate the matrix element for a local potential in coordinate space as

$$\langle\vec{R'}|V|\vec{R}\rangle = \delta(\vec{R'} - \vec{R})V(\vec{R}), \tag{2.39}$$

where $V(\vec{R})$ is given by

$$V(\vec{R}) \equiv (2\pi)^D \lambda \delta(\vec{R}). \tag{2.40}$$

Then substituting this potential in equation (2.39) we have

$$\begin{aligned} \langle \vec{R}'|V|\vec{R}\rangle &= (2\pi)^D \lambda \delta(\vec{R}' - \vec{R})\delta(\vec{R}) \\ &= (2\pi)^D \lambda \delta(\vec{R}')\delta(\vec{R}). \end{aligned} \tag{2.41}$$

In this way we see that the Dirac-$\delta$ potential is a local and separable. Now we need this potential projected in a momentum space in order to find the form factor that is defined in this space, then we write the matrix elements of Dirac-$\delta$ potential in a momentum space $\langle \vec{p'}|V|\vec{p}\rangle$ as

$$\begin{aligned} \langle \vec{p'}|V|\vec{p}\rangle &= \langle \vec{p'}| \left\{ \int d^D R' |\vec{R'}\rangle\langle\vec{R'}| \right\} V \left\{ \int d^D R |\vec{R}\rangle\langle\vec{R}| \right\} |\vec{p}\rangle \\ &= \int d^D R' d^D R \langle \vec{p'}|\vec{R'}\rangle \langle \vec{R'}|V|\vec{R}\rangle \left\langle \vec{R}\,|\vec{p}\right\rangle \\ &= \int d^D R' d^D R \frac{1}{(2\pi)^{D/2}} e^{-i\vec{p'}.\vec{R'}} \langle \vec{R'}|V|\vec{R}\rangle \frac{1}{(2\pi)^{D/2}} e^{i\vec{p}.\vec{R}} \\ &= \int d^D R' d^D R \frac{1}{(2\pi)^{D/2}} e^{-i\vec{p'}.\vec{R'}} (2\pi)^D \lambda \delta(\vec{R'})\delta(\vec{R}) \frac{1}{(2\pi)^{D/2}} e^{i\vec{p}.\vec{R}} \\ &= \lambda \int d^D R'\ d^D R\ e^{-i\vec{p'}.\vec{R'}} e^{i\vec{p}.\vec{R}} \delta(\vec{R'})\delta(\vec{R}) \\ &= \lambda g^*(\vec{p'}) g(\vec{p}) \end{aligned} \tag{2.42}$$

where $g(\vec{p}) = \int d^D R\ e^{i\vec{p}.\vec{R}} \delta(\vec{R}) = 1$.

### 2.2.1 Renormalization

The form factor of the Dirac-$\delta$ potential in equation (2.38) introduce a divergence in the integral for larger momentum. In 2D and 3D the divergence can be treated by introducing a physical scale in the problem[39]. We will follow the theoretical development presented in F. F. Bellotti doctoral thesis [40]. The physical information is introduced by attributing a physical value, $\lambda_R$, for the T-matrix in a subtraction energy point, $E = \mu^2_{(2)}$ (the index here indicates that we are considering the two-body scale), that means

$$\tau_R(-\mu^2_{(2)}) = \lambda_R(-\mu^2_{(2)}) \tag{2.43}$$

the index $R$ means renormalization. This is a general method used both for two and three -body systems [41, 42, 43].
Introducing the above condition (physical information) in equation (2.38) and the form factor as 1, we obtain

$$\tau_R(-\mu_{(2)}^2) = \left[\lambda^{-1} - \int d^D p \frac{1}{-\mu_{(2)}^2 - \frac{p^2}{2m_{red}}}\right]^{-1} = \lambda_R(-\mu_{(2)}^2),$$
$$\lambda^{-1} - \int d^D p \frac{1}{-\mu_{(2)}^2 - \frac{p^2}{2m_{red}}} = {\lambda_R}^{-1}(-\mu_{(2)}^2),$$
$$\lambda^{-1} = {\lambda_R}^{-1}(-\mu_{(2)}^2) + \int d^D p \frac{1}{-\mu_{(2)}^2 - \frac{p^2}{2m_{red}}}. \tag{2.44}$$

and substituting (2.44) into the equation (2.38), we get a finite expression for the transition matrix of two-body system

$$\begin{aligned} \tau_R^{-1}(E) &= {\lambda_R}^{-1}(-\mu_{(2)}^2) + \int d^D p \left[\frac{1}{-\mu_{(2)}^2 - \frac{p^2}{2m_{red}}} - \frac{1}{E - \frac{p^2}{2m_{red}} + i\epsilon}\right] \\ &= {\lambda_R}^{-1}(-\mu_{(2)}^2) + (E + \mu_{(2)}^2) \int d^D p \frac{1}{\left(-\mu_{(2)}^2 - \frac{p^2}{2m_{red}}\right)\left(E - \frac{p^2}{2m_{red}} + i\epsilon\right)}. \end{aligned} \tag{2.45}$$

the integral part in equation (2.45) is now finite. Using the residue theorem to calculate the integral, the renormalized two-body T-matrix in 2D (with D=2) is given by

$$\tau_R(E)^{-1} = \lambda_R^{-1}(-\mu_{(2)}^2) - 4\pi m_{red} \ln\left(\sqrt{\frac{-E}{\mu_{(2)}^2}}\right), \tag{2.46}$$

this equation could be used for positives energies (scattering states, $E > 0$) and negatives energies (binding states, $E < 0$). We just need to be careful, when we are in the case of the scattering states, the scattering amplitude is obtained from the analytic continuation of the equation (2.46) in the upper complex semi-plane of $E$ as shown in the next equation.

$$\tau_R(E)^{-1} = \lambda_R^{-1}(-\mu_{(2)}^2) - 4\pi m_{red} \ln\left(\sqrt{\frac{E}{\mu_{(2)}^2}}\right) + 2\pi^2 i m_{red}, \tag{2.47}$$

If we are looking at the matrix elements of the equation (2.46), it is not straightforward to identify the $s$-wave scattering phase-shift and cross-section for the zero-range model, and it was pointed out in the reference [27]. In units of $\hbar = 2m_{red} = 1$, the matrix elements for the two-body transition matrix in the case of $E > 0$ written as $\langle p'|T(E)|p\rangle = 2\pi\langle \vec{p'}|T(E)|\vec{p}\rangle$ are

$$\langle p'|T(E)|p\rangle = \frac{2\pi}{\lambda_R^{-1}(-\mu_{(2)}^2) - \pi \ln\left(\sqrt{\frac{E}{\mu_{(2)}^2}}\right) + i\pi^2}$$

$$= \frac{2}{\pi(-\cot(\delta_2) + i)} \tag{2.48}$$

where the $s$-wave scattering phase-shift for the zero-range model is defined as

$$\cot(\delta_2) = -\frac{1}{\pi^2\lambda(-\mu_{(2)}^2)} + \frac{1}{\pi}\ln\left(\frac{E}{\mu_{(2)}^2}\right) \tag{2.49}$$

and the two-dimensional scattering length $a_2$ is found to be

$$\bar{a} = -\frac{1}{\pi^2\lambda(-\mu_{(2)}^2)} + \frac{1}{\pi}\ln(\mu_{(2)}^2) = a_2 + \frac{1}{\pi}\ln(\mu_{(2)}^2) \tag{2.50}$$

as we see in this equation, the logarithmic term, which appears in the low energy expansion, lead us to an ambiguity in the definition of the scattering length in 2D, which depends on the scale used to measure the energy. To avoid this ambiguity, the binding energy of the pair, $E_b$, is chosen as the physical scale in the problem. This means we can choose the subtraction point $\mu_{(2)}^2$ to be the physical scale of the problem, $\mu_{(2)}^2 = -E_b$, and at the same time this choice is going to fix the value of the physical information, given by $\lambda(-\mu_{(2)}^2)$, therefore

$$\tau_R(E)^{-1} = \lambda_R^{-1}(E_b) - 4\pi m_{red}\ln\left(\sqrt{\frac{E}{E_b}}\right), \tag{2.51}$$

at the bound-state pole, case ($E < 0$)

$$\lambda_R^{-1}(E_b) = 0. \tag{2.52}$$

Finally, the renormalized 2D two-body T-matrix for the zero-range model is

$$\tau_R(E)^{-1} = -4\pi m_{red}\ln\left(\sqrt{\frac{-E}{E_b}}\right), \tag{2.53}$$

which is used to describe some properties in the case of three-body systems in 2D.

## 2.3 Three-body T-Matrix for Dirac-$\delta$ potential

As we know the transition operator is given by equation (2.1), this relation also holds for a case of N-particles, then for the case of three-body system where we have three distinguishable particles called A, B, C, where the interaction between particles is given by $V$, the three-body transition operator is written as

$$T(E) = V + VG^{(\pm)}V \tag{2.54}$$

and using the relation between the total Green function and the free Green function, equation (2.27) we obtain

$$T(E) = (1 + T(E)G_0^{(+)}(E))V = V(1 + G_0^{(+)}(E)T(E)). \tag{2.55}$$

If we use a separable Dirac-$\delta$ potential, which we already probed that beside to be local is a separable potential, equation (2.41). Then we may write the potential as

$$V = \lambda|\vec{\chi}\rangle\langle\vec{\chi}| = \lambda\{|\chi_1\rangle\langle\chi_1| + |\chi_2\rangle\langle\chi_2| + |\chi_3\rangle\langle\chi_3|\} = v_A + v_B + v_C \tag{2.56}$$

where $\lambda$ as before is the potential strength, the $v_A$, $v_B$ and $v_C$ are the separable potential where $v_A$ mean that the particles B and C are interacting, $v_B$ mean that the particles A and C are interacting and $v_C$ mean that the particles A and B are interacting.

Replacing the potential into the transition operator, equation (2.55), we get

$$T(E) = v_A + v_B + v_C + (v_A + v_B + v_C)G_0^{(+)}(E)T(E). \tag{2.57}$$

## 2.4 The Faddeev Equations

It has been known from the literature that the Lippmann-Schwinger equation for three or more bodies has two main problems to solve this kind of system. The first problem noticed by severals authors [29, 30, 31] is that the Lippmann-Schwinger integral equation does not have a unique solution. Specially in ref [30] they show the existence of a solution to the homogenous counterpart of the Lippmann-Schwinger integral equation.

The second problem arises from the analysis of the kernel given by $K \equiv G_0V$. Faddeev [32] pointed out that this kernel is not square integrable ($\mathcal{L}^2$), which basically means that by integrating this quantity over all space, in this case two dimensions, the integral tends to infinity. The same problem was also studied by other authors, e.g. Weinberg [33], where he expressed the trouble of the Lippmann-Schwinger integral equation in a number of ways: **1)** The Kernel of the Lippmann-Schwinger equation is not of the Hilbert-Schmidt (or $\mathcal{L}^2$) type, even if the interactions are well enough behaved to give an $\mathcal{L}^2$ two-particle kernel. **2)** The L-S kernel has a continuous spectrum. **3)** The graphs for the L-S kernel are not connected. **4)** The scattering amplitudes are not meromorphic functions of the coupling constant, but contain cuts, as well as the poles which are present for two particles. **5)** The "Fredholm alternative" does not hold.

Until now the most successfully solution to this problem has been provide by Faddeev[32, 34] who has suggested the following method, we will follow the theoretical development in the Charles J. Joachain [38], where the basic idea is to write the scattering operator $T(E)$ as

$$T(E) = T^{(1)}(E) + T^{(2)}(E) + T^{(3)}(E) \tag{2.58}$$

where $T^{(1)}(E)$ represent the sum of al the diagrams contributing to $T(E)$ in which particles 2 and 3 are going to interact. In other words, $T^{(1)}(E)$ is a scattering operator such that any three-body process has occurred (including no interaction at all), and then particles 2 and 3 interact.

In order to understand, let's introduce a diagrammatic representation [38], which is quite intuitive and may help to visualize some of the key properties for three-body systems.

1. Particles are represented by horizontal lines, which in the beginning of the line the particles are going to be labelled by $\vec{p'}_i$, and after some process occur, in the end of the line the particles are labelled by $\vec{p}_i$.

2. A vertical dashed line between a pair of lines corresponds to a two-body interaction.

3. The $T$-matrix is represented by a shaded blob.

4. There is a propagator $G_0$ between two vertical dashed lines or a dashed line and a $T$-matrix in the same diagram.

Considering the equation (2.29), which is $T = V + VG_0T$. Then, replacing $V = V^1 + V^2 + V^3$ we have

$$\begin{aligned} T &= V + VG_0T \\ &= V^1 + V^2 + V^3 + (V^1 + V^2 + V^3)G_0T \\ &= V^3 + V^1 + V^2 + V^3G_0T + V^1G_0T + V^2G_0T. \end{aligned}$$

and the diagrammatic Faddeev decomposition is

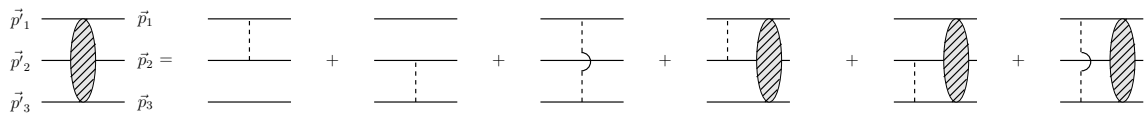


Figura 2.3: Diagrammatic Faddeev decomposition for the three-body $T$-matrix. The diagrams where one particle remains unaffected, are called disconnected.

Now that we know how the diagrams work, we return to the equation (2.58) and using the Faddeev idea we may draw the different terms of the scattering operator, $T(E) = T^{(1)}(E) + T^{(2)}(E) + T^{(3)}(E)$, as

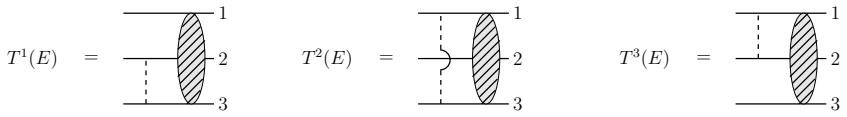


Figura 2.4: Diagrammatic representation of equation (2.58)

where in a more carefully analysis of the content of $T^{(1)}(E)$ from the figure above, allows us to separate it in two parts. In the first part, the particle 1 never interacts with particles 2 and 3. Due to that, we are able to write as a two-body scattering operator, shown in the figure (2.5) ( **we will call $t_1(E)$ as the two-body $T$-matrix**)

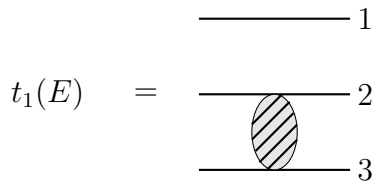


Figura 2.5: Diagrammatic representation first part of the term $T^{(1)}(E)$, whose equation is $t_1(E)$

In the second part, there are an arbitrary sequence of interactions between the three particles, followed by an interaction between particles 1 and 3 ( or 1 and 2 ), and then particles 2 and 3 interact a certain number of times. The sum of such contributions may be represented as

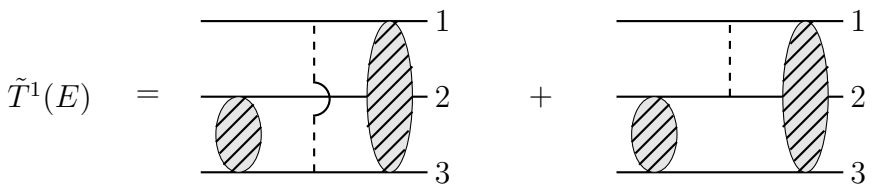


Figura 2.6: Diagrammatic representation second part of the term $T^{(1)}(E)$, whose equation is $\tilde{T}^{(1)}(E) = t_1 G_0 T^{(2)} + t_1 G_0 T^{(3)}$

all contribution to the first term of equation (2.58) is

$$\begin{aligned} T^{(1)} &= t_1 + \tilde{T}^{(1)} \\ &= t_1 + t_1 G_0 T^{(2)} + t_1 G_0 T^{(3)} \end{aligned} \tag{2.59}$$

in a similar way, we may find the second and third terms of equation (2.58)

$$T^{(2)} = t_2 + t_2 G_0 T^{(1)} + t_2 G_0 T^{(3)} \tag{2.60}$$

and

$$T^{(3)} = t_3 + t_3 G_0 T^{(1)} + t_3 G_0 T^{(2)}. \tag{2.61}$$

The equations (2.59, 2.60 and 2.61 ) are known as the Faddeev equations for the T-operator. In matrix form they are written as

$$\begin{pmatrix} T^{(1)} \\ T^{(2)} \\ T^{(3)} \end{pmatrix} = \begin{pmatrix} t_1 \\ t_2 \\ t_3 \end{pmatrix} + \begin{pmatrix} 0 & t_1 & t_1 \\ t_2 & 0 & t_2 \\ t_3 & t_3 & 0 \end{pmatrix} G_0 \begin{pmatrix} T^{(1)} \\ T^{(2)} \\ T^{(3)} \end{pmatrix}. \tag{2.62}$$

The Faddeev equations, obtained from the diagrammatic representation must be the same as obtained directly from the two and three -body transition operators, as follows.By using the transition operator definition, equation (2.57), of a three-body system with a separable potential $V = V^1 + V^2 + V^3$, and replacing the Faddeev decomposition we get

$$\begin{aligned} T(E) &= V^1 + V^2 + V^3 + (V^1 + V^2 + V^3) G_0 T(E) \\ T^{(1)}(E) + T^{(2)}(E) + T^{(3)}(E) &= V^1 + V^2 + V^3 + (V^1 + V^2 + V^3) G_0 T(E) \end{aligned} \tag{2.63}$$

where we can define that

$$T^{(1)}(E) = V^1 + V^1 G_0 T(E) \tag{2.64}$$
$$T^{(2)}(E) = V^2 + V^2 G_0 T(E) \tag{2.65}$$
$$T^{(3)}(E) = V^3 + V^3 G_0 T(E) \tag{2.66}$$

in order to find a relation with the two-body transition operator we use the equation (2.33) where we are denoting $t_1$ as the two-body transition operator where only particles 2 and 3 interacts with a potential $V^1$, $t_2$ as the two-body transition operator where only particles 1 and 3 interacts with a potential $V^2$ and $t_3$ as the two-body transition operator where only particles 1 and 2 interacts with a potential $V^3$, then the two-body transition operators are written as

$$t_1 = V^1 + t_1 G_0 V^1 \tag{2.67}$$
$$t_2 = V^2 + t_2 G_0 V^2 \tag{2.68}$$
$$t_3 = V^3 + t_3 G_0 V^3 \tag{2.69}$$

replacing equation (2.67) into the equation (2.64) we obtain

$$\begin{aligned} T^{(1)}(E) &= t_1 - t_1 G_0 V^1 + (t_1 - t_1 G_0 V^1) G_0 T(E) \\ &= t_1 + t_1 G_0 T(E) - t_1 G_0 (V^1 + V^1 G_0 T(E)) \\ &= t_1 + t_1 G_0 T(E) - t_1 G_0 T^{(1)}(E) \\ &= t_1 + t_1 G_0 (T(E) - T^{(1)}(E)) \\ &= t_1 + t_1 G_0 (T^{(1)}(E) + T^{(2)}(E) + T^{(3)}(E) - T^{(1)}(E)) \\ &= t_1 + t_1 G_0 (T^{(2)}(E) + T^{(3)}(E)) \end{aligned} \tag{2.70}$$

following the same procedure for $T^{(2)}(E)$ and $T^{(3)}(E)$ we may find the next equations

$$T^{(2)}(E) = t_2 + t_2 G_0 (T^{(1)}(E) + T^{(3)}(E)), \tag{2.71}$$
$$T^{(3)}(E) = t_3 + t_3 G_0 (T^{(1)}(E) + T^{(2)}(E)), \tag{2.72}$$

where if we wrote in matrix form we get the same equations as obtained from the diagrammatic procedure

$$\begin{pmatrix} T^{(1)} \\ T^{(2)} \\ T^{(3)} \end{pmatrix} = \begin{pmatrix} t_1 \\ t_2 \\ t_3 \end{pmatrix} + \begin{pmatrix} 0 & t_1 & t_1 \\ t_2 & 0 & t_2 \\ t_3 & t_3 & 0 \end{pmatrix} G_0 \begin{pmatrix} T^{(1)} \\ T^{(2)} \\ T^{(3)} \end{pmatrix}.$$

Then from the above equation, that is the same as equation (2.62), it have a similar form of equation (2.57), then we may say that the Kernel matrix is given by

$$K = VG_0 = \begin{pmatrix} 0 & t_1 & t_1 \\ t_2 & 0 & t_2 \\ t_3 & t_3 & 0 \end{pmatrix} G_0 \tag{2.73}$$

Analyzing the equation (2.62), they explicitly depend of the well behaved two-body transition operator. This suggests that something has been gained by introducing the Faddeev method. More specifically, Faddeev proved that this kernel (2.73) $[K] \equiv K_{ij}\,(i,j=1,2,3)$ is square integrable $\mathcal{L}^2$ for all physical values of the energy $(E)$ [35]. Even better he showed that for real values of $E$, the fifth power of the kernel is a compact operator [36, 37], that basically mean the solution of the Faddeev equation is unique.

The kernel, equation (2.73), it seems to be disconnected and by disconnected we mean that it not have interaction connected by a propagator, an example of a connected terms is $(t_1 G_0 t_2)$, but iterating once the Faddeev equations (2.62), we get the new matrices equations that contains $[K^2]$

$$\begin{aligned} \begin{pmatrix} T^{(1)} \\ T^{(2)} \\ T^{(3)} \end{pmatrix} &= \begin{pmatrix} t_1 \\ t_2 \\ t_3 \end{pmatrix} + \begin{pmatrix} 0 & t_1 & t_1 \\ t_2 & 0 & t_2 \\ t_3 & t_3 & 0 \end{pmatrix} G_0 \left[ \begin{pmatrix} t_1 \\ t_2 \\ t_3 \end{pmatrix} + \begin{pmatrix} 0 & t_1 & t_1 \\ t_2 & 0 & t_2 \\ t_3 & t_3 & 0 \end{pmatrix} G_0 \begin{pmatrix} T^{(1)} \\ T^{(2)} \\ T^{(3)} \end{pmatrix} \right] \\ \begin{pmatrix} T^{(1)} \\ T^{(2)} \\ T^{(3)} \end{pmatrix} &= \begin{pmatrix} t_1 \\ t_2 \\ t_3 \end{pmatrix} + [K] \begin{pmatrix} t_1 \\ t_2 \\ t_3 \end{pmatrix} + [K^2] \begin{pmatrix} T^{(1)} \\ T^{(2)} \\ T^{(3)} \end{pmatrix} \end{aligned} \tag{2.74}$$

with

$$[K^2] = \begin{bmatrix} t_1 G_0 t_2 + t_1 G_0 t_3 & t_1 G_0 t_3 & t_1 G_0 t_2 \\ t_2 G_0 t_3 & t_2 G_0 t_1 + t_2 G_0 t_3 & t_2 G_0 t_1 \\ t_3 G_0 t_2 & t_3 G_0 t_1 & t_3 G_0 t_1 + t_3 G_0 t_2 \end{bmatrix} G_0 \tag{2.75}$$

we see that this new kernel $[K^2]$ only contains connected elements. Then by remembering the troubles mentioned by Weinberg [33], specifically the third problem, where he mentioned that the L-S kernel are not connected, it is not a problem anymore.

Once we obtained the Faddeev equations and they seem to be consistent without the problems that the Lippmann-Schwinger equation have, we are able to write the Faddeev equations in momentum space by using the equation (2.29), since this way we may see the matrix elements of the transition operator for a three-body system in a transition from a state $|\vec{p_i}\vec{p_j}\vec{p_k}\rangle$ to an state $|\vec{p_i'}\vec{p_j'}\vec{p_k'}\rangle$, that are going to be useful in the computation of the spectator function. Then by replacing the

definition of the green's function from (2.1) and the matrix elements of the two-body interaction potential $\langle \vec{p'}_i \vec{p'}_j \vec{p'}_k | V^i | \vec{p}_i \vec{p}_j, \vec{p}_k \rangle = \delta(\vec{p'}_i - \vec{p}_i) \langle \vec{p'}_j \vec{p'}_k | V^i | \vec{p}_j \vec{p}_k \rangle$ into the two-body transition operator we have

$$\begin{aligned}
\langle \vec{p'}_i \vec{p'}_j \vec{p'}_k | t_i(E) | \vec{p}_i \vec{p}_j \vec{p}_k \rangle = \quad & \delta(\vec{p'}_i - \vec{p}_i) \langle \vec{p'}_j \vec{p'}_k | V^i | \vec{p}_j \vec{p}_k \rangle \\
& + \delta(\vec{p'}_i - \vec{p}_i) \int \Bigg[ d\vec{p''}_j d\vec{p''}_k \langle \vec{p'}_j \vec{p'}_k | V^i | \vec{p''}_j \vec{p''}_k \rangle \\
& \times \frac{1}{E - p_i^2/2m_i - p_j^{''2}/2m_j - p_k^{''2}/2m_k + i\epsilon} \\
& \times \langle \vec{p''}_j \vec{p''}_k | t_i(E - p_i^2/2m_i) | \vec{p}_j \vec{p}_k \rangle \Bigg] \qquad (2.76)
\end{aligned}$$

where this equation is known as the two-body transition matrix element in the three-body Hilbert space. If we replace $\vec{q}_i = \vec{p}_j \vec{p}_k$, we are able to write a short expression for equation (2.76)

$$\begin{aligned}
\langle \vec{p'}_i, \vec{p'}_j \vec{p'}_k | t_i(E) | \vec{p}_i, \vec{p}_j \vec{p}_k \rangle &= \delta(\vec{p'}_i - \vec{p}_i) \left\langle \vec{p'}_j \vec{p'}_k \left| t_i \left( E - \frac{p_i^2}{2m_i} \right) \right| \vec{p}_j \vec{p}_k \right\rangle \\
&= \delta(\vec{p'}_i - \vec{p}_i) \left\langle \vec{q'}_i \left| t_i \left( E - \frac{p_i^2}{2m_i} \right) \right| \vec{q}_i \right\rangle \qquad (2.77)
\end{aligned}$$

and replacing it into the Faddeev equations 2.59, 2.60 and 2.61 we get

$$\begin{aligned}
& \left\langle \vec{p'}_1 \vec{p'}_2 \vec{p'}_3 \left| T^{(1)}(E) \right| \vec{p}_1 \vec{p}_2 \vec{p}_3 \right\rangle \\
& = \delta(\vec{p'}_1 - \vec{p}_1) \left\langle \vec{q'}_1 \left| t_1 \left( E - p_1^2/2m_1 \right) \right| \vec{q}_1 \right\rangle + \int d\vec{p''}_1 d\vec{p''}_2 d\vec{p''}_3 \delta(\vec{p'}_1 - \vec{p''}_1) \\
& \times \left\langle \vec{q'}_1 \left| t_1 \left( E - p_1^{''2}/2m_1 \right) \right| \vec{q''}_1 \right\rangle \frac{1}{E - \sum_{i=1}^3 p_i^{''2}/2m_i + i\epsilon} \delta(\vec{p_1} + \vec{p_2} + \vec{p_3} - \vec{p_1''} - \vec{p_2''} - \vec{p_3''}) \\
& \times \left[ \left\langle \vec{p''}_1 \vec{p''}_2 \vec{p''}_3 \left| T^{(2)}(E) \right| \vec{p}_1 \vec{p}_2 \vec{p}_3 \right\rangle + \left\langle \vec{p''}_1 \vec{p''}_2 \vec{p''}_3 \left| T^{(3)}(E) \right| \vec{p}_1 \vec{p}_2 \vec{p}_3 \right\rangle \right]. \qquad (2.78)
\end{aligned}$$

In a similar way we may find in momentum space the equations for $T^{(2)}(E)$ and $T^{(3)}(E)$. In equation (2.78) we see that all the information about the two-body subsystems which is necessary in order to solve the Faddeev equations, appears in the form of the two-body matrices $t_i$. We may say that those two-body $T$-matrix play a similar role to the interaction potentials in two-body scattering. Usually the two-body $T$-matrix elements are more closely related to experiment than the potentials $V^i$, and become more significantly when the potential are not known. Another important property of the Faddeev equations in three-body system is that the matrix $T^{(i)}(E)$ satisfies the unitarity if the two-body $T$-matrices satisfy the unitarity [32].

## 2.5 Three-body bound state equation in 2D

The dynamics of three-body system with a short-range potential can be describe by the set of equations (2.62). That may allow us to say that $T$-matrix gives information about both, bound ($E_3 < 0$) and scattering ($E_3 > 0$) states. In order to find the three-body bound state equations in two dimensions, we will focus in negative energies, where starting from the transition operator we will be able to derive the coupled homogenous integral equations for the bound state. There is another procedure using directly the Faddeev decomposition for the bound-state wave function [44].

Using a completeness relation of a set of eigenstates of the Hamiltonian $H = H_0 + V$, defined as

$$\hat{1} = \sum_B |\Phi_B\rangle\langle\Phi_B| + \int dk^2 |\Psi_c^{(+)}\rangle\langle\Psi_c^{(+)}| \tag{2.79}$$

where $|\Phi_B\rangle$ represents the wave function of bound states and $|\Psi_c^{(+)}\rangle$ the wave function of scattering states. There are eigenfunction of $H$ with eigenvalues $E_B$ and $E_c$. Inserting equation (2.79) into the three-body transition operator (2.1), we get

$$\begin{aligned}
T(E_3) &= V + VG\hat{1}V \\
T(E_3) &= V + VG\left[\sum_B |\Phi_B\rangle\langle\Phi_B| + \int dk^2 |\Psi_c^{(+)}\rangle\langle\Psi_c^{(+)}|\right] V \\
T(E_3) &= V + V\frac{1}{E_3 - H + i\epsilon}\left[\sum_B |\Phi_B\rangle\langle\Phi_B| + \int dk^2 |\Psi_c^{(+)}\rangle\langle\Psi_c^{(+)}|\right] V \\
T(E_3) &= V + \sum_B \frac{V|\Phi_B\rangle\langle\Phi_B|V}{E_3 - E_B + i\epsilon} + \int dk^2 \frac{V|\Psi_c^{(+)}\rangle\langle\Psi_c^{(+)}|V}{E_3 - E_c + i\epsilon}
\end{aligned} \tag{2.80}$$

where we can identify the bound-state poles of the transition operator. When the three-body system is close to a bound state ($E_3 \approx E_B$), the second term on the right-hand-side of equation (2.80) become dominant due to the proximity of the pole and the scattering term can be neglected. Defining the bound-state vertex function as

$$|\Gamma_B\rangle = V|\Phi_B\rangle, \tag{2.81}$$

we may rewrite the three-body $T$-matrix near the pole ($E_3 \approx E_B$), where the first and third term in the right-hand-side of equation (2.80) are neglected, as

$$T(E_3) \approx \frac{|\Gamma_B\rangle\langle\Gamma_B|}{E_3 - E_B} = \frac{|\Gamma_B\rangle\langle\Gamma_B|}{E_3 + |E_B|} \tag{2.82}$$

we are able to decompose this $T$-matrix in three Faddeev components as we did ($T(E_3) = T^{(1)}(E_3) + T^{(2)}(E_3) + T^{(3)}(E_3)$) in equation (2.58), replacing the potential, $V = V^1 + V^2 + V^3$ we have

$$T_a(E_3) \approx \frac{|\Gamma_a\rangle\langle\Gamma_B|}{E_3 + |E_B|}, \tag{2.83}$$

where $|\Gamma_a\rangle = V^a|\Phi_B\rangle$, with $a = 1, 2, 3$. Equation (2.83) is the transition operator of a three-body system when we are really close to the energy of a bound-state.

### 2.5.1 The Spectator Functions near to the bound-state ($E_3 \approx E_B$) pole

Now that we found the $a$-component of the Faddeev equation (2.83), we are able to introduce it into the $T$-matrix component of the Faddeev equation that we found in **Section (2.4)**, specifically in equation (2.62). But first let decompose that $T$-matrix of the Faddeev equations into an index equation in order to find the $a$-component

$$T^{(a)}(E_3) = t_a(E_2^R)\left\{1 + G_0(E_3 + i\epsilon)\left(T^{(b)}(E_3) + T^{(c)}(E_3)\right)\right\} \tag{2.84}$$

where $a, b, c = 1, 2, 3$ follow a cyclical permutation and $(a \neq b \neq c)$. We should note that the argument of the two-body transition operator is indeed the relative two-body energy ($E_2^R$, the superscript $R$ is to denote Relative between the particles that are interacting and the subscript 2 is for the two-body bound energy), then we must relate this energy $E_2^R$ with the three-body bounding energy $E_3$ and that can be done by using the Jacobi coordinates of a three-body system (Appendix B).

In the framework of the two-body system, the total two-body energy $E_2^T$, connects with the relative two-body energy through

$$E_2^T = E_2^R + \frac{q_2^2}{2(m_b + m_c)} \tag{2.85}$$

where $q_2$ is the total momentum of the pair.

In the framework of the C.M. of the three-body energy $E_3$, the total energy of the pair is the difference between the three-body energy and the kinetic energy of the third particle, namely $E_2^T = E_3 - \frac{q_1^2}{2m_a}$.

Then by using an auxiliary momentum $Q$, which we will see it in details in the next chapter, then if $Q = 0$, the momentum of the pair is exactly the momentum of the third particle. In other words, $|\vec{q_1}| = |-\vec{q_2}| = q$ [40], then the relative two-body energy as function of the three-body energy is written as

$$E_2^R = E_3 - \frac{q^2}{2m_a} - \frac{q^2}{2(m_b + m_c)} = E_3 - \frac{q^2}{2m_{bc,a}} \tag{2.86}$$

replacing the relative two-body energy found in equation (2.86) into the equation (2.84)

$$T^{(a)}(E_3) = t_a\left(E_3 - \frac{q_a^2}{2m_{bc,a}}\right)\left\{1 + G_0(E_3 + i\epsilon)\left(T^{(b)}(E_3) + T^{(c)}(E_3)\right)\right\}. \tag{2.87}$$

Finally we found the $a$-component of the Faddeev equation, now we continue by replacing as we mention the $a$-component of the tree-body transition operator near to a bound state ($T_a(E_3) \approx \frac{|\Gamma_a\rangle\langle\Gamma_B|}{E_3+|E_B|}$)

$$\frac{|\Gamma_a\rangle\langle\Gamma|}{E_3+|E_a|} \approx t_{R_a}\left(E_3 - \frac{q_a^2}{2m_{bc,a}}\right)\left[1 + \left(G_0^{(+)}(E_3)\right)\left(\frac{|\Gamma_b\rangle\langle\Gamma|}{E_3+|E_a|} + \frac{|\Gamma_c\rangle\langle\Gamma|}{E_3+|E_a|}\right)\right] \tag{2.88}$$

where $E_a$ is the bound-state energy from the pair $(bc)$. Remembering that this equation is valid for $(E_3 \to -|E_a|)$, and becoming in a homogenous equation, which reads

$$|\Gamma_a\rangle = t_{R_a}\left(E_3 - \frac{q_a^2}{2m_{bc,a}}\right)\left(G_0^{(+)}(E_3)\right)\left(|\Gamma_b\rangle + |\Gamma_c\rangle\right) \tag{2.89}$$

replacing explicitly the two-body $T$-matrix from equation (2.36) we get

$$|\Gamma_a\rangle = |\chi_a\rangle\tau_R\left(E_3 - \frac{q_a^2}{2m_{bc,a}}\right)\langle\chi_a|\left(G_0^{(+)}(E_3)\right)\left(|\Gamma_b\rangle + |\Gamma_c\rangle\right) \tag{2.90}$$

and the projection of equation (2.90) into states $|\vec{p}_a, \vec{q}_a\rangle$ is

$$\langle\vec{p}_a, \vec{q}_a|\Gamma_a\rangle = \langle\vec{p}_a|\chi_a\rangle\tau_R\left(E_3 - \frac{q_a^2}{2m_{bc,a}}\right)\langle\chi_a, \vec{q}_a|\left(G_0^{(+)}(E_3)\right)\left(|\Gamma_b\rangle + |\Gamma_c\rangle\right) \tag{2.91}$$

for a Dirac-$\delta$ potential, we are able to write $\langle\vec{p}_a, \vec{q}_a|\Gamma_a\rangle = \langle\vec{p}_a|\chi_a\rangle\langle\vec{q}_a|f_a\rangle = g_a(\vec{p}_a)f_a(\vec{q}_a) = f_a(\vec{q}_a)$, (we already show that the form factor for a Dirac-$\delta$ potential $g_a(\vec{p}_a) = 1$, equation 2.42). Then the spectator function or the $a$-component from the homogenous Faddeev equation for three-body bound state is given by

$$f_a(\vec{q}_a) = \tau_R\left(E_3 - \frac{q_a^2}{2m_{bc,a}}\right)\langle\chi_a, \vec{q}_a|\left(G_0^{(+)}(E_3)\right)\left(|\Gamma_b\rangle + |\Gamma_c\rangle\right) \tag{2.92}$$

we may remind that the spectator functions describe the relation of each spectator particle with corresponding two-body subsystem. By permutation of the index $a = i, j, k$ that are the particles labelled in Appendix (B), we are able to found the other spectator functions $f_i$, $f_j$ and $f_k$, where all of them satisfy a set of three coupled homogenous integral equations when the interaction between particles is through a zero-range potential. If we base our study of three-body system in cases such as: 1) three identical particles, then just one spectator function has to be solved as the spectator functions are all equals $f_i = f_j = f_k$. 2) Two identical and one different, then we will solve a set of two coupled homogeneous integral equation since $f_i = f_j \neq f_k$. 3) A general case where the three particles are distinguishable, we get a set of coupling equations as

$$f_i(\vec{q}_i) = \tau_R\left(E_3 - \frac{q_i^2}{2m_{jk,i}}\right)\langle\chi_i, \vec{q}_i|\left(G_0^{(+)}(E_3)\right)\left(|\chi_j\rangle|f_j\rangle + |\chi_k\rangle|f_k\rangle\right) \tag{2.93}$$

$$f_j(\vec{q}_j) = \tau_R\left(E_3 - \frac{q_j^2}{2m_{ki,j}}\right)\langle\chi_j,\vec{q}_j|\left(G_0^{(+)}(E_3)\right)(|\chi_i\rangle|f_i\rangle + |\chi_k\rangle|f_k\rangle) \tag{2.94}$$

$$f_k(\vec{q}_k) = \tau_R\left(E_3 - \frac{q_k^2}{2m_{ij,k}}\right)\langle\chi_k,\vec{q}_k|\left(G_0^{(+)}(E_3)\right)(|\chi_i\rangle|f_i\rangle + |\chi_j\rangle|f_j\rangle) \tag{2.95}$$

Replacing explicitly the matrix elements from the two-body $T$-matrix and calculating the matrix elements for the free Green function in the different basis $\langle\chi_i,\vec{q}_i|\left(G_0^{(+)}(E_3)\right)|\chi_j\rangle|f_j\rangle$ (made in details in the Appendix C), we finally get the set of three coupled homogenous integral equations for the bound state of a three-body system composed by distinguishable particles as (the particles are denoted by the index $i,j,k$ while the internal momentum is labeled by uppercase $K$)

$$\begin{aligned} f_i(\vec{q}_i) = &\left[-4\pi\frac{m_jm_k}{m_j+m_k}\ln\left(\sqrt{\frac{\frac{m_i+m_j+m_k}{2m_i(m_j+m_k)}q_i^2 - E_3}{E_{jk}}}\right)\right]^{-1} \\ &\times\left[\int d^2K\frac{f_j(\vec{K})}{E_3 - \frac{m_i+m_k}{2m_im_k}q_i^2 - \frac{m_j+m_k}{2m_jm_k}K^2 - \frac{1}{m_k}\vec{K}\cdot\vec{q}_i}\right. \\ &\left.+\int d^2K\frac{f_j(\vec{K})}{E_3 - \frac{m_i+m_j}{2m_im_j}q_i^2 - \frac{m_j+m_k}{2m_jm_k}K^2 - \frac{1}{m_j}\vec{K}\cdot\vec{q}_i}\right], \end{aligned} \tag{2.96}$$

$$\begin{aligned} f_j(\vec{q}_j) = &\left[-4\pi\frac{m_im_k}{m_i+m_k}\ln\left(\sqrt{\frac{\frac{m_i+m_j+m_k}{2m_j(m_i+m_k)}q_j^2 - E_3}{E_{ik}}}\right)\right]^{-1} \\ &\times\left[\int d^2K\frac{f_i(\vec{K})}{E_3 - \frac{m_j+m_k}{2m_jm_k}q_j^2 - \frac{m_i+m_k}{2m_im_k}K^2 - \frac{1}{m_k}\vec{K}\cdot\vec{q}_j}\right. \\ &\left.+\int d^2K\frac{f_k(\vec{K})}{E_3 - \frac{m_i+m_j}{2m_im_j}q_j^2 - \frac{m_i+m_k}{2m_im_k}K^2 - \frac{1}{m_i}\vec{K}\cdot\vec{q}_j}\right], \end{aligned} \tag{2.97}$$

$$\begin{aligned} f_k(\vec{q}_k) = &\left[-4\pi\frac{m_im_j}{m_i+m_j}\ln\left(\sqrt{\frac{\frac{m_i+m_j+m_k}{2m_k(m_i+m_j)}q_k^2 - E_3}{E_{ij}}}\right)\right]^{-1} \\ &\times\left[\int d^2K\frac{f_i(\vec{K})}{E_3 - \frac{m_j+m_k}{2m_jm_k}q_k^2 - \frac{m_i+m_j}{2m_im_j}K^2 - \frac{1}{m_j}\vec{K}\cdot\vec{q}_k}\right. \\ &\left.+\int d^2K\frac{f_j(\vec{K})}{E_3 - \frac{m_i+m_k}{2m_im_k}q_k^2 - \frac{m_i+m_j}{2m_im_j}K^2 - \frac{1}{m_i}\vec{K}\cdot\vec{q}_k}\right]. \end{aligned} \tag{2.98}$$

The two-body boun state energy of each pair, defined as the scale factor of the two-body system, is labeled as $E_{ij}$, $E_{jk}$, $E_{ik}$.

### 2.5.2 Wave Function of Three-body bound-states

Using the spectator functions from equations (2.96, 2.97, 2.98), the vertex function $|\Gamma_B\rangle = V|\Phi_B\rangle$, defined in equation (2.81), a separable and local potential $V = v_i + v_j + v_k$ and a general bound state $|\Psi_B\rangle$, its possible to combine those to write

$$\begin{aligned} V|\Psi_B\rangle &= |\Gamma_i\rangle + |\Gamma_j\rangle + |\Gamma_k\rangle \\ (v_i + v_j + v_k)|\Psi_B\rangle &= |\Gamma_i\rangle + |\Gamma_j\rangle + |\Gamma_k\rangle \end{aligned} \tag{2.99}$$

multiplying by the free Green function on both sides we have

$$|\Psi_{ijk}\rangle = |\Psi_i\rangle + |\Psi_j\rangle + |\Psi_k\rangle = G_0(E_3)\left[|\Gamma_i\rangle + |\Gamma_j\rangle + |\Gamma_k\rangle\right] \tag{2.100}$$

where $|\Psi_i\rangle = G_0(E_3)v_i|\Psi_B\rangle$ is one of the Faddeev components of the wave function. Now projecting into the Jacobi momenta $|\vec{p},\vec{q}\rangle$

$$\langle\vec{p}_i,\vec{q}_i|\Psi_{ijk}\rangle = \langle\vec{p}_i,\vec{q}_i|G_0(E_3)\left(|\Gamma_i\rangle + |\Gamma_j\rangle + |\Gamma_k\rangle\right) \tag{2.101}$$

once again, replacing ($|\Gamma_i\rangle = |\chi_j\rangle|f_j\rangle$) and the matrix elements of $\langle\chi_i,\vec{q}_i|(G_0^{(+)}(E_3))|\chi_j\rangle|f_j\rangle$ obtained in details at the Appendix C, we get

$$\Psi_{ijk}(\vec{q}_i,\vec{p}_i) = \frac{f_i(\vec{q}_i) + f_j(\vec{q}_j(\vec{q}_i,\vec{p}_i)) + f_k(\vec{q}_k(\vec{q}_i,\vec{p}_i))}{E_3 - \frac{m_i+m_j+m_k}{2m_i(m_j+m_k)}q_i^2 - \frac{m_j+m_k}{2m_jm_k}p_i^2} \tag{2.102}$$

if we use a compact notation such as $(\alpha,\beta,\gamma)$ that are cyclic permutations on the particles $(i,j,k)$ and introducing this notation into the wave function, taking into account the Jacobi relative momentum of particle $\alpha$ to the C.M. of the subsystem $(\beta\gamma)$, we may write

$$\Psi(\vec{q}_\alpha,\vec{p}_\alpha) = \frac{f_\alpha(q_\alpha) + f_\beta\left(\left|\vec{p}_\alpha - \frac{m_\beta}{m_\beta+m_\gamma}\vec{q}_\alpha\right|\right) + f_\gamma\left(\left|\vec{p}_\alpha + \frac{m_\gamma}{m_\beta+m_\gamma}\vec{q}_\alpha\right|\right)}{-E_3 + \frac{q_\alpha^2}{2m_{\beta\gamma,\alpha}} + \frac{p_\alpha^2}{2m_{\beta\gamma}}}, \tag{2.103}$$

the Jacobi momenta of a particle $\alpha(q_\alpha,p_\alpha)$ with shifted arguments are given in the Appendix C, $m_{\beta\gamma,\alpha} = m_\alpha(m_\beta+m_\gamma)/(m_\alpha+m_\beta+m_\gamma)$ and $m_{\beta\gamma} = (m_\beta m_\gamma)/(m_\beta+m_\gamma)$. Using this formalism we can write the spectator functions in a compact notation as

$$\begin{aligned} f_\alpha(\vec{q}) = &\left[4\pi m_{\beta\gamma}\ln\left(\sqrt{\frac{\frac{q_\alpha^2}{2m_{\beta\gamma,\alpha}} - E_3}{E_{\beta\gamma}}}\right)\right]^{-1} \\ &\times\int d^2K\left(\frac{f_\beta(\vec{K})}{-E_3 + \frac{q^2}{2m_{\alpha\gamma}} + \frac{K^2}{2m_{\beta\gamma}} + \frac{1}{m_\gamma}\vec{K}\cdot\vec{q}} + \frac{f_\gamma(\vec{K})}{-E_3 + \frac{q^2}{2m_{\alpha\beta}} + \frac{K^2}{2m_{\beta\gamma}} + \frac{1}{m_\beta}\vec{K}\cdot\vec{q}}\right). \end{aligned} \tag{2.104}$$

In order to solve this integral for the spectator functions, we will assume that the particles are interacting by $s$-wave potentials and the total angular momentum is zero. Thus, the spectator functions do not depend on the angle that means $f_\alpha(\vec{q}) \equiv f_\alpha(q)$. Remembering that we wrote in polar coordinate the vector $\vec{K}$ as we see in Figure (2.1), then, the angular integration on equation (2.104) is solved using

$$\int_0^{2\pi} \frac{d\theta}{1 - z\cos(\theta)} = \frac{1}{\sqrt{(1-z^2)}}, \tag{2.105}$$

where the constant $z$ satisfies $|z| < 1$. Then, the spectator functions are written as

$$f_\alpha(\vec{q}) = 2\pi \left[ 4\pi m_{\beta\gamma} \ln \left( \sqrt{\frac{\frac{q_\alpha^2}{2m_{\beta\gamma,\alpha}} - E_3}{E_{\beta\gamma}}} \right) \right]^{-1}$$
$$\times \int_0^\infty dK \left( \frac{K f_\beta(K)}{\sqrt{\left(-E_3 + \frac{q^2}{2m_{\alpha\gamma}} + \frac{K^2}{2m_{\beta\gamma}}\right)^2 - \left(\frac{Kq}{m_\gamma}\right)^2}} + \frac{K f_\gamma(K)}{\sqrt{\left(-E_3 + \frac{q^2}{2m_{\alpha\beta}} + \frac{K^2}{2m_{\beta\gamma}}\right)^2 - \left(\frac{Kq}{m_\beta}\right)^2}} \right) \tag{2.106}$$

where $(\alpha, \beta\gamma = i, j, k)$ follow a cyclical permutation of the particles. The study of three-body bound states, will be based on the numerical solution of the coupled homogeneous integral equations for the spectator functions given by equation (2.106).

# Chapter 3

# Structure of three-body system in 2D

In this chapter, we describe the formalism used to calculate the mean square radii defined for a general three-body system compounded by three distinguishable particles. The Jacobi coordinate momenta are showed in Figure 3.1.

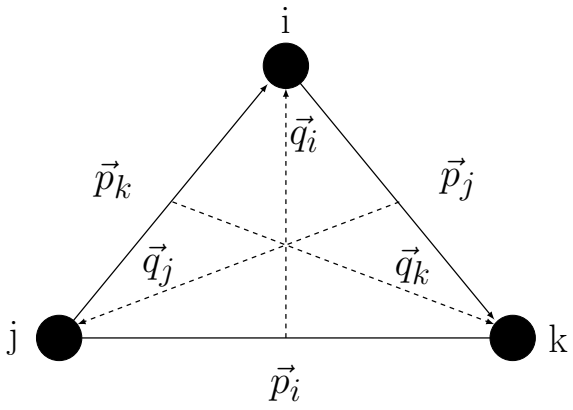


Figura 3.1: Jacobi momenta.

## 3.1 Mean Square Radii

From the Figure 3.1 we may distinguish three sets of Jacobi coordinates that help us to describe each particles, in other words for the particle $i$ they relatives Jacobi coordinates are ($\vec{p}_i$ and $\vec{q}_i$) with the canonically conjugate positions ($\vec{R}_i$ and $\vec{r}_i$) respectively.

The mean square radius, can be calculated for any pair of particles ($\langle r^2_{ij}\rangle$, $\langle r^2_{jk}\rangle$, $\langle r^2_{ik}\rangle$) and the mean square radius from each particle to the center-of-mass of the three-body system ($\langle r^2_{i_{CM}}\rangle$, $\langle r^2_{j_{CM}}\rangle$, $\langle r^2_{k_{CM}}\rangle$).

The mean square radius from the relative distance between particles $j$ and $k$, $\langle R^2_i\rangle \equiv \langle r^2_{jk}\rangle$, is given as

$$\langle R_i^2 \rangle = \int d^2 R_i R_i^2 \rho_i(R_i) \tag{3.1}$$

where the two-body matter density is given by

$$\rho_i(R_i) = \int d^2 r_i |\psi(\vec{r}_i, \vec{R}_i)|^2. \tag{3.2}$$

Using a Fourier transform, we may write the two-body matter density as

$$\rho_i(R_i) = \int d^2 Q F_{jk}(Q^2) \frac{e^{-i\vec{Q}.\vec{R}_i}}{(2\pi)^2} \tag{3.3}$$

and the inverse Fourier transform give us the function $F_{jk}(Q^2)$, which must be normalized by $F_{jk}(0) \equiv 1$

$$F_{jk}(Q^2) = \int d^2 R_i e^{i\vec{Q}.\vec{R}_i} \rho_i(R_i) \tag{3.4}$$

expanding the exponential in the equation (3.4) in a Taylor series until second order we get

$$e^{i\vec{Q}.\vec{R}_i} \approx 1 + (i\vec{Q}.\vec{R}_i) + \frac{(i\vec{Q}.\vec{R}_i)^2}{2!} \tag{3.5}$$

and replacing back into the equation (3.4) we have

$$F_{jk}(Q^2) \approx \int d^2 R_i \rho_i(R_i) + \int d^2 R_i (i\vec{Q}.\vec{R}_i) \rho_i(R_i) + \int d^2 R_i \frac{(i\vec{Q}.\vec{R}_i)^2}{2!} \rho_i(R_i) \tag{3.6}$$

but if we considerer a spherical symmetry for $\rho_i(R_i)$ and that the integration of the probability function over all space is one

- $\int d^2 R_i \rho_i(R_i) = 1$
- $\int d^2 R_i (i\vec{Q}.\vec{R}_i) \rho_i(R_i) = 0$

$$\begin{aligned}
F_{jk}(Q^2) \approx \quad & 1 - \frac{1}{2} \int d^2 R_i (Q_\alpha R_i^\alpha)(Q_\beta R_i^\beta) \rho_i(R_i) \\
\approx \quad & 1 - \frac{1}{2} (Q_\alpha Q_\beta) \int d^2 R_i (R_i^\alpha R_i^\beta) \rho_i(R_i) \\
\approx \quad & 1 - \frac{1}{2} (Q_\alpha Q_\beta) \int d^2 R_i (\frac{\delta_{\alpha\beta}}{2} R_i^\alpha R_i^\beta) \rho_i(R_i) \\
\approx \quad & 1 - \frac{1}{4} (Q^2) \int d^2 R_i \, R_i^2 \rho_i(R_i) \\
\approx \quad & 1 - \frac{Q^2}{4} \langle R_i^2 \rangle,
\end{aligned} \tag{3.7}$$

where if we perform a derivation of the equation (3.7) against $Q^2$ we get

$$\langle R_i^2 \rangle = -4 \frac{dF_i(Q^2)}{dQ^2}\bigg|_{Q^2=0}. \tag{3.8}$$

As we mentioned before, by following the same procedure we showed, its possible to obtain

$$\langle R_j^2 \rangle \equiv \langle r_{ik}^2 \rangle = -4 \frac{dF_j(Q^2)}{dQ^2}\bigg|_{Q^2=0} \tag{3.9}$$

$$\langle R_k^2 \rangle \equiv \langle r_{ij}^2 \rangle = -4 \frac{dF_k(Q^2)}{dQ^2}\bigg|_{Q^2=0}. \tag{3.10}$$

Now applying a similar procedure, (we just need to be careful over the coordinate we are integrating) we can find the mean square radius from a particle to the center-of-mass of the three-body system.

The mean square radius from the relative distance between a particles $i$ and the center-of-mass of the pair $(j,k)$ is given as

$$\langle r_i^2 \rangle = \int d^2 r_i r_i^2 \rho_i(r_i) \tag{3.11}$$

where the one-body matter density is given by

$$\rho_i(r_i) = \int d^2 R_i |\psi(\vec{r}_i, \vec{R}_i)|^2. \tag{3.12}$$

Using a Fourier transform, we write the one-body matter density as

$$\rho_i(r_i) = \int d^2 Q F_i(Q^2) \frac{e^{-i\vec{Q}.\vec{r}_i}}{(2\pi)^2} \tag{3.13}$$

and the inverse Fourier transformation give us the function $F_i(Q^2)$, which must be normalized by $F_i(0) \equiv 1$

$$F_i(Q^2) = \int d^2 r_i e^{i\vec{Q}.\vec{r}_i} \rho_i(r_i) \tag{3.14}$$

expanding the exponential in the equation (3.14) in a Taylor series until second order we get

$$e^{i\vec{Q}.\vec{r}_i} \approx 1 + (i\vec{Q}.\vec{r}_i) + \frac{(i\vec{Q}.\vec{r}_i)^2}{2!} \tag{3.15}$$

and replacing back into the equation (3.14) we have

$$F_i(Q^2) \approx \int d^2 r_i \rho_i(r_i) + \int d^2 r_i (i\vec{Q}.\vec{r}_i) \rho_i(r_i) + \int d^2 r_i \frac{(i\vec{Q}.\vec{r}_i)^2}{2!} \rho_i(r_i) \tag{3.16}$$

but if we considerer a spherical symmetry for $\rho_i(r_i)$ and that the integration of the probability function over all space is one

- $\int d^2r_i\rho_i(r_i) = 1$
- $\int d^2r_i(i\vec{Q}.\vec{r}_i)\rho_i(r_i) = 0$

$$\begin{aligned} F_i(Q^2) \approx & \quad 1 - \frac{1}{2}\int d^2r_i(Q_\alpha r_i^\alpha)(Q_\beta r_i^\beta)\rho_i(r_i) \\ \approx & \quad 1 - \frac{1}{2}(Q_\alpha Q_\beta)\int d^2r_i(r_i^\alpha r_i^\beta)\rho_i(r_i) \\ \approx & \quad 1 - \frac{1}{2}(Q_\alpha Q_\beta)\int d^2r_i(\frac{\delta_{\alpha\beta}}{2}r_i^\alpha r_i^\beta)\rho_i(r_i) \\ \approx & \quad 1 - \frac{1}{4}(Q^2)\int d^2r_i\, r_i^2\rho_i(r_i) \\ \approx & \quad 1 - \frac{Q^2}{4}\langle r_i^2\rangle, \end{aligned} \tag{3.17}$$

where if we perform a derivation of the equation (3.17) against $Q^2$ we get

$$\langle r_i^2\rangle = -4\frac{dF_i(Q^2)}{dQ^2}\bigg|_{Q^2=0}. \tag{3.18}$$

It is necessary to find the center-of-mass of the three-body system that is located in the line that connect the particle $(i)$ and the center-of-mass of the pair $(jk)$

$$\langle r_{i_{CM}}^2\rangle = -4\left(\frac{m_j + m_k}{m_i + m_j + m_k}\right)\frac{dF_i(Q^2)}{dQ^2}\bigg|_{Q^2=0}, \tag{3.19}$$

the other two mean square radius from particles to the center-of-mass of the three-body system can be found in a similar procedure.

## 3.2 Function $F(Q^2)$ in Momentum Space

The auxiliary functions $F(Q^2)$ are given by equations (3.4) and (3.14). Thus, writing explicitly the Fourier transform we have

$$\begin{aligned} F(Q^2) &= \int d^2r_i e^{i\vec{Q}.\vec{r}_i}\left[\int d^2R_i\,|\psi|^2\right] \\ &= \int d^2r_i e^{i\vec{Q}.\vec{r}_i}\int d^2R_i\langle\vec{r}_i,\vec{R}_i|\psi\rangle\langle\psi|\vec{r}_i,\vec{R}_i\rangle \\ &= \int d^2r_i e^{i\vec{Q}.\vec{r}_i}\int d^2R_i d^2p_i d^2q_i d^2p'_i d^2q'_i\Big[\langle\vec{r}_i,\vec{R}_i|\vec{p}_i,\vec{q}_i\rangle\langle\vec{p}_i,\vec{q}_i|\psi\rangle \\ &\qquad \times\langle\psi|\vec{p'}_i,\vec{q'}_i\rangle\langle\vec{p'}_i,\vec{q'}_i|\vec{r}_i,\vec{R}_i\rangle\Big], \end{aligned} \tag{3.20}$$

replacing

$$\langle \vec{r}_i, \vec{R}_i | \vec{p}_i, \vec{q}_i \rangle = \frac{1}{2\pi} e^{i\vec{r}_i \cdot \vec{p}_i} \times \frac{1}{2\pi} e^{i\vec{R}_i \cdot \vec{q}_i} \tag{3.21}$$

into equation (3.20) and using the definition of the Dirac delta function

$$\begin{aligned} F(Q^2) \quad &= \frac{1}{(2\pi)^2} \int d^2 r_i d^2 R_i d^2 p_i d^2 q_i d^2 p'_i d^2 q'_i e^{i(\vec{Q}+\vec{p}_i-\vec{p'}_i)\cdot\vec{r}_i} e^{i(\vec{q}_i-\vec{q'}_i)\cdot\vec{R}_i} \\ &\quad \times \langle \vec{p}_i, \vec{q}_i | \psi \rangle \langle \psi | \vec{p'}_i, \vec{q'}_i \rangle \\ &= \int d^2 p_i d^2 q_i d^2 p'_i d^2 q'_i \ \delta(Q + p_i - p'_i) \delta(q_i - q'_i) \\ &\quad \times \langle \vec{p}_i, \vec{q}_i | \psi \rangle \langle \psi | \vec{p'}_i, \vec{q'}_i \rangle \\ &= \int d^2 p_i d^2 q_i \ \langle \vec{p}_i, \vec{q}_i | \psi \rangle \left\langle \psi | \vec{p'}_i + \vec{Q}, \vec{q'}_i \right\rangle \end{aligned}$$

then if the wave function is real

- $\langle \vec{p}_i, \vec{q}_i | \psi \rangle = \langle \vec{p}_i, \vec{q}_i | \psi \rangle^*$
- $\left\langle \psi | \vec{p'}_i + \vec{Q}, \vec{q'}_i \right\rangle = \left\langle \psi | \vec{p'}_i + \vec{Q}, \vec{q'}_i \right\rangle^*$

for numerical convenience we can symmetrize the arguments of those wave function by substituting the momentum $\vec{p}_i$ by $\vec{p}_i - \frac{\vec{Q}}{2}$,

$$F(Q^2) = \int d^2 q_i d^2 p_i \left\langle \vec{q}_i, \vec{p}_i + \frac{\vec{Q}}{2} \middle| \psi \right\rangle \left\langle \vec{q}_i, \vec{p}_i - \frac{\vec{Q}}{2} \middle| \psi \right\rangle . \tag{3.22}$$

As we see, our function $F(Q^2)$ is given by the wave function from equation (2.103), which at the same time depends on the Jacobi coordinates we choose to project, that means we are going to have six different functions $F(Q^2)$ such as ($F_{ij}(Q^2)$, $F_{jk}(Q^2)$ and $F_{ki}(Q^2)$) for the mean square radii between particles and ($F_i(Q^2)$, $F_j(Q^2)$ and $F_k(Q^2)$) for the particle and the center-of-mass of the three-body system. Note that here the arguments of the wave functions are given in shifted momenta due to the introduction of an auxiliary momentum $Q^2$.

## 3.3 Radii of three-body system

From the above sections we already have the expressions for the different radii in a three-body system, equations (3.8,3.9,3.10 and 3.19) and the equation (3.22) give us the auxiliary function $F(Q^2)$ necessary to compute the different radii. Also this equation have an angular dependence on the integrals which we can see in figure 3.2

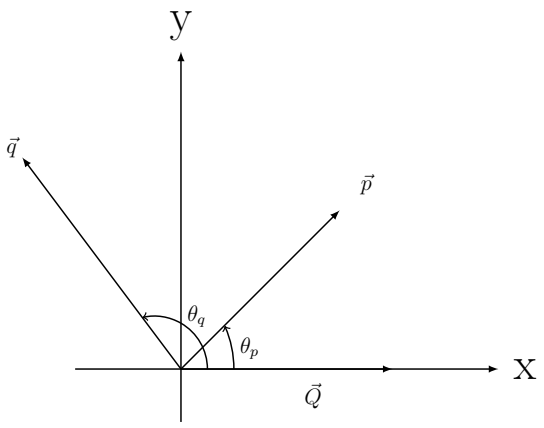


Figura 3.2: Momenta orientation. $\vec{Q}$ is fixed in $X$ axis.

Additionally, we will change the particles name as: $i \equiv A$, $j \equiv B$ and $k \equiv C$, with masses $m_i$, $m_j$ and $m_k$, respectively. In the next equations $\mathcal{A} = m_j/m_k$ and $\mathcal{B} = m_i/m_k$.

### 3.3.1 Radius between particles B and C

From equation (3.8) using the new notation we get

$$\langle R_i^2 \rangle \equiv \langle r_{BC}^2 \rangle = -4 \frac{dF_{BC}(Q^2)}{dQ^2}\bigg|_{Q^2=0} \tag{3.23}$$

where $F_{BC}(Q^2)$ is described by the Jacobi relative momentum $\vec{p}_i$ and $\vec{q}_i$

$$F_{BC}(Q^2) = \int d^2q_i d^2p_i \left\langle \vec{q}_i, \vec{p}_i + \frac{\vec{Q}}{2} \middle| \psi \right\rangle \left\langle \vec{q}_i, \vec{p}_i - \frac{\vec{Q}}{2} \middle| \psi \right\rangle \tag{3.24}$$

with

$$\begin{aligned} \Psi(\vec{q}_i, \vec{p}_i) &= \frac{f_i(q_i) + f_j\left(\left|\vec{p}_i - \frac{m_j}{m_j+m_k}\vec{q}_i\right|\right) + f_k\left(\left|\vec{p}_i + \frac{m_k}{m_j+m_k}\vec{q}_i\right|\right)}{|E_3| + H_0(\vec{p}_i, \vec{q}_i)} \\ &= \frac{f_{BC}(q_i) + f_{AC}\left(\left|\vec{p}_i - \frac{m_j}{m_j+m_k}\vec{q}_i\right|\right) + f_{AB}\left(\left|\vec{p}_i + \frac{m_k}{m_j+m_k}\vec{q}_i\right|\right)}{|E_3| + H_0(\vec{p}_i, \vec{q}_i)} \end{aligned} \tag{3.25}$$

and replacing the wave function (3.25) into the equation (3.24), taking into account the shifted arguments on the momentums

$$F_{BC}(Q^2) = \int dq_i d\theta_q dp_i d\theta_p \left[ \frac{f_{BC}(q_i) + f_{AC}\left(\left|\vec{p}_i + \frac{\vec{Q}}{2} - \frac{\mathcal{A}}{\mathcal{A}+1}\vec{q}_i\right|\right) + f_{AB}\left(\left|\vec{p}_i + \frac{\vec{Q}}{2} + \frac{1}{\mathcal{A}+1}\vec{q}_i\right|\right)}{|E_3| + H_0(\vec{p}_i + \frac{\vec{Q}}{2}, \vec{q}_i)} \right.$$

$$\times \frac{f_{BC}(q_i) + f_{AC}\left(\left|\vec{p}_i - \frac{\vec{Q}}{2} - \frac{\mathcal{A}}{\mathcal{A}+1}\vec{q}_i\right|\right) + f_{AB}\left(\left|\vec{p}_i - \frac{\vec{Q}}{2} + \frac{1}{\mathcal{A}+1}\vec{q}_i\right|\right)}{|E_3| + H_0(\vec{p}_i - \frac{\vec{Q}}{2}, \vec{q}_i)}\Bigg]. \quad (3.26)$$

The shifted momenta arguments are calculated in (Appendix D).

### 3.3.2 Radius between particles A and C

From equation (3.9) using the new notation we get

$$\langle r_j^2 \rangle \equiv \langle r_{AC}^2 \rangle = -4 \frac{dF_{AC}(Q^2)}{dQ^2}\bigg|_{Q^2=0} \quad (3.27)$$

where $F_{AC}(Q^2)$ is described by the Jacobi relative momentum $\vec{p}_j$ and $\vec{q}_j$

$$F_{AC}(Q^2) = \int d^2q_j d^2p_j \left\langle \vec{q}_j, \vec{p}_j + \frac{\vec{Q}}{2}\middle|\psi\right\rangle \left\langle \vec{q}_j, \vec{p}_j - \frac{\vec{Q}}{2}\middle|\psi\right\rangle \quad (3.28)$$

with

$$\begin{aligned} \Psi(\vec{q}_j, \vec{p}_j) &= \frac{f_j(q_j) + f_k\left(\left|\vec{p}_j - \frac{m_k}{m_k+m_i}\vec{q}_j\right|\right) + f_i\left(\left|\vec{p}_j + \frac{m_i}{m_k+m_i}\vec{q}_j\right|\right)}{|E_3| + H_0(\vec{p}_j, \vec{q}_j)} \\ &= \frac{f_{AC}(q_j) + f_{AB}\left(\left|\vec{p}_j - \frac{m_k}{m_k+m_i}\vec{q}_j\right|\right) + f_{BC}\left(\left|\vec{p}_j + \frac{m_i}{m_k+m_i}\vec{q}_j\right|\right)}{|E_3| + H_0(\vec{p}_j, \vec{q}_j)} \end{aligned} \quad (3.29)$$

and replacing the wave function (3.29) into the equation (3.28), taking into account the shifted arguments on the momenta

$$\begin{aligned} F_{AC}(Q^2) = \int dq_j d\theta_q dp_j d\theta_p \Bigg[ & \frac{f_{AC}(q_j) + f_{AB}\left(\left|\vec{p}_j + \frac{\vec{Q}}{2} - \frac{1}{\mathcal{B}+1}\vec{q}_j\right|\right) + f_{BC}\left(\left|\vec{p}_j + \frac{\vec{Q}}{2} + \frac{\mathcal{B}}{\mathcal{B}+1}\vec{q}_j\right|\right)}{|E_3| + H_0(\vec{p}_j + \frac{\vec{Q}}{2}, \vec{q}_j)} \\ & \times \frac{f_{AC}(q_j) + f_{AB}\left(\left|\vec{p}_j - \frac{\vec{Q}}{2} - \frac{1}{\mathcal{B}+1}\vec{q}_j\right|\right) + f_{BC}\left(\left|\vec{p}_j - \frac{\vec{Q}}{2} + \frac{\mathcal{B}}{\mathcal{B}+1}\vec{q}_j\right|\right)}{|E_3| + H_0(\vec{p}_j - \frac{\vec{Q}}{2}, \vec{q}_j)}\Bigg]. \end{aligned} \quad (3.30)$$

### 3.3.3 Radius between particles A and B

From equation (3.10) using the new notation we get

$$\langle r_k^2 \rangle \equiv \langle r_{AB}^2 \rangle = -4 \frac{dF_{AB}(Q^2)}{dQ^2}\bigg|_{Q^2=0} \quad (3.31)$$

where $F_{AB}(Q^2)$ is described by the Jacobi relative momenta $\vec{p}_k$ and $\vec{q}_k$

$$F_{AB}(Q^2) = \int d^2q_k d^2p_k \left\langle \vec{q}_k, \vec{p}_k + \frac{\vec{Q}}{2}\middle|\psi\right\rangle \left\langle \vec{q}_k, \vec{p}_k - \frac{\vec{Q}}{2}\middle|\psi\right\rangle \quad (3.32)$$

with

$$\begin{aligned}\Psi(\vec{q}_k,\vec{p}_k) &= \frac{f_k(q_k)+f_i\left(\left|\vec{p}_k-\frac{m_i}{m_i+m_j}\vec{q}_k\right|\right)+f_j\left(\left|\vec{p}_k+\frac{m_j}{m_i+m_j}\vec{q}_k\right|\right)}{|E_3|+H_0(\vec{p}_k,\vec{q}_k)} \\ &= \frac{f_{AB}(q_k)+f_{BC}\left(\left|\vec{p}_k-\frac{m_i}{m_i+m_j}\vec{q}_k\right|\right)+f_{AC}\left(\left|\vec{p}_k+\frac{m_j}{m_i+m_j}\vec{q}_k\right|\right)}{|E_3|+H_0(\vec{p}_k,\vec{q}_k)} \quad (3.33)\end{aligned}$$

and replacing the wave function (3.33) into the equation (3.32), taking into account the shifted arguments on the momentum

$$\begin{aligned}F_{AB}(Q^2) = \int dq_k d\theta_q dp_k d\theta_p \Bigg[ &\frac{f_{AB}(q_k)+f_{BC}\left(\left|\vec{p}_k+\frac{\vec{Q}}{2}-\frac{\mathcal{B}}{\mathcal{A}+\mathcal{B}}\vec{q}_k\right|\right)+f_{AC}\left(\left|\vec{p}_k+\frac{\vec{Q}}{2}+\frac{\mathcal{A}}{\mathcal{A}+\mathcal{B}}\vec{q}_k\right|\right)}{|E_3|+H_0(\vec{p}_k+\frac{\vec{Q}}{2},\vec{q}_k)} \\ &\times\frac{f_{AB}(q_k)+f_{BC}\left(\left|\vec{p}_k-\frac{\vec{Q}}{2}-\frac{\mathcal{B}}{\mathcal{A}+\mathcal{B}}\vec{q}_k\right|\right)+f_{AC}\left(\left|\vec{p}_k-\frac{\vec{Q}}{2}+\frac{\mathcal{A}}{\mathcal{A}+\mathcal{B}}\vec{q}_k\right|\right)}{|E_3|+H_0(\vec{p}_k-\frac{\vec{Q}}{2},\vec{q}_k)}\Bigg]. \quad (3.34)\end{aligned}$$

### 3.3.4 Radius between particle A, B and C and the Center of Mass of the System

The mean square radii from particles A, B and C to the C.M. of the three-body system are computed by their respective form factors, which are given by

$$\langle r_A^2\rangle \equiv \left(\frac{m_j+m_k}{m_i+m_j+m_k}\right)\langle r_i^2\rangle = -4\left(\frac{m_j+m_k}{m_i+m_j+m_k}\right)\left.\frac{dF_A(Q^2)}{dQ^2}\right|_{Q^2=0} \quad (3.35)$$

$$F_A(Q^2) = \int d^2q_i d^2p_i \left\langle \vec{q}_i+\frac{\vec{Q}}{2},\vec{p}_i\middle|\psi\right\rangle\left\langle \vec{q}_i-\frac{\vec{Q}}{2},\vec{p}_i\middle|\psi\right\rangle,$$

$$\langle r_B^2\rangle \equiv \left(\frac{m_i+m_k}{m_i+m_j+m_k}\right)\langle r_j^2\rangle = -4\left(\frac{m_i+m_k}{m_i+m_j+m_k}\right)\left.\frac{dF_B(Q^2)}{dQ^2}\right|_{Q^2=0} \quad (3.36)$$

$$F_B(Q^2) = \int d^2q_j d^2p_j \left\langle \vec{q}_j+\frac{\vec{Q}}{2},\vec{p}_j\middle|\psi\right\rangle\left\langle \vec{q}_j-\frac{\vec{Q}}{2},\vec{p}_j\middle|\psi\right\rangle,$$

and

$$\langle r_C^2\rangle \equiv \left(\frac{m_i+m_j}{m_i+m_j+m_k}\right)\langle r_k^2\rangle = -4\left(\frac{m_i+m_j}{m_i+m_j+m_k}\right)\left.\frac{dF_C(Q^2)}{dQ^2}\right|_{Q^2=0} \quad (3.37)$$

$$F_C(Q^2) = \int d^2q_k d^2p_k \left\langle \vec{q}_k+\frac{\vec{Q}}{2},\vec{p}_k\middle|\psi\right\rangle\left\langle \vec{q}_k-\frac{\vec{Q}}{2},\vec{p}_k\middle|\psi\right\rangle.$$

# Chapter 4

# Numerical Method and Results

The homogeneous integral equations for the spectator functions in equation (2.106) are a set of coupled equation, which do not have analytic solution in general. Then it turns into a numerical problem which exist many solution methods for solving an integral equation in literature, some of them are found in reference [46, 47].

The three-body problem by this analysis consists in finding the bound-state energy from an integral equation. Those energies arise from the zeros of a determinant of the matrix. Consequently the spectator functions can be calculate replacing the already founded values of the bound-state energies. As soon as the energies and spectator functions are determined we are able to calculate the wave function and therefore the mean square radii of the system.

## 4.1 Three-body energy

We are going to illustrate a method by using a three-body system ABC formed by distinguishable bosons. Their masses are $m_A = m_C = 1$ and $m_B$ is a variable mass. For simplicity we will assume that the two-body binding energies are equal and given by $E_{AB} = E_{AC} = E_{BC} = E_2 = 1$.

By using the Gaussian Quadrature we integrate over orthogonal polynomial approximation to the integrand defined at specially located points or nodes. The nodes are chosen to give the exact value of a polynomial of the highest possible degree.

This method require the location of the nodes which are given by the roots of the Legendre polynomial of degree n. Since the orthogonal property of Legendre polynomials exists only on the interval $-1 \leq x \leq 1$.

Writing in a compact form the set of equations (2.106) using $E_3 \equiv \frac{E_3'}{E_2}$ and $q \equiv \frac{q'}{\sqrt{mE_2}}$

$$f_\alpha(q) = \int_0^\infty K_{\alpha\beta}(E_3; q, k) f_\beta(k) dk + \int_0^\infty K_{\alpha\gamma}(E_3; q, k) f_\gamma(k) dk \,, \tag{4.1}$$

where $(\alpha = A, B, C)$ goes in a cyclical permutation. Expanding explicitly for each particle the above equation, we get the set of equation as

$$f_A(q) = \int_0^\infty K_{12}(E_3; q, k) f_B(k) dk + \int_0^\infty K_{13}(E_3; q, k) f_C(k) dk \,, \tag{4.2}$$

$$f_B(q) = \int_0^\infty K_{21}(E_3; q, k) f_A(k) dk + \int_0^\infty K_{23}(E_3; q, k) f_C(k) dk \,, \tag{4.3}$$

$$f_C(q) = \int_0^\infty K_{31}(E_3; q, k) f_A(k) dk + \int_0^\infty K_{32}(E_3; q, k) f_B(k) dk \,, \tag{4.4}$$

with the kernels defined as

$$K_{12}(E_3; q, k) = \frac{\left[2m_{BC} \ln\left(\sqrt{\frac{\frac{q^2}{2m_{BC,A}} - E_3}{E_{BC}}}\right)\right]^{-1} k}{\sqrt{\left(-E_3 + \frac{q^2}{2m_{AC}} + \frac{k^2}{2m_{BC}}\right)^2 - \left(\frac{kq}{m_C}\right)^2}} \,, \tag{4.5}$$

$$K_{13}(E_3; q, k) = \frac{\left[2m_{BC} \ln\left(\sqrt{\frac{\frac{q^2}{2m_{BC,A}} - E_3}{E_{BC}}}\right)\right]^{-1} k}{\sqrt{\left(-E_3 + \frac{q^2}{2m_{AB}} + \frac{k^2}{2m_{BC}}\right)^2 - \left(\frac{kq}{m_B}\right)^2}} \,, \tag{4.6}$$

$$K_{21}(E_3; q, k) = \frac{\left[2m_{AC} \ln\left(\sqrt{\frac{\frac{q^2}{2m_{AC,B}} - E_3}{E_{AC}}}\right)\right]^{-1} k}{\sqrt{\left(-E_3 + \frac{q^2}{2m_{BC}} + \frac{k^2}{2m_{AC}}\right)^2 - \left(\frac{kq}{m_C}\right)^2}} \,, \tag{4.7}$$

$$K_{23}(E_3; q, k) = \frac{\left[2m_{AC} \ln\left(\sqrt{\frac{\frac{q^2}{2m_{AC,B}} - E_3}{E_{AC}}}\right)\right]^{-1} k}{\sqrt{\left(-E_3 + \frac{q^2}{2m_{AB}} + \frac{k^2}{2m_{AC}}\right)^2 - \left(\frac{kq}{m_A}\right)^2}} \,, \tag{4.8}$$

$$K_{31}(E_3; q, k) = \frac{\left[2m_{AB} \ln\left(\sqrt{\frac{\frac{q^2}{2m_{AB,C}} - E_3}{E_{AB}}}\right)\right]^{-1} k}{\sqrt{\left(-E_3 + \frac{q^2}{2m_{BC}} + \frac{k^2}{2m_{AB}}\right)^2 - \left(\frac{kq}{m_B}\right)^2}} \,, \tag{4.9}$$

$$K_{32}(E_3; q, k) = \frac{\left[2m_{AB} \ln\left(\sqrt{\frac{\frac{q^2}{2m_{AB,C}} - E_3}{E_{AB}}}\right)\right]^{-1} k}{\sqrt{\left(-E_3 + \frac{q^2}{2m_{AC}} + \frac{k^2}{2m_{AB}}\right)^2 - \left(\frac{kq}{m_A}\right)^2}} . \tag{4.10}$$

Then the Gauss-Legendre mesh-points are used for the discretization of the kernels in equations 4.5 to 4.10, where the discrete momentum $q_i \equiv x_i$ corresponds to a set points with its respective Gauss-Legendre weights $dq_i \equiv \omega_i$. The limits on the integral equation from the spectator functions are defined to be in the interval $[0, \infty]$. It is possible to use a transformation of the Gauss-Legendre mesh points and weights in order to be defined over this interval as

$$q_i = \frac{1+x_i}{1-x_i} \tag{4.11}$$

$$w_i = \frac{2}{(1-x_i)^2}\omega_i \tag{4.12}$$

therefore, the discretization of the integral equations (4.1) is written as

$$\begin{aligned}
f_\alpha(q_i) &= \sum_{j=1}^{N} K_{\alpha\beta}(E_3, q_i, q_j) f_\beta(q_j) w_j + \sum_{j=1}^{N} K_{\alpha\gamma}(E_3, q_i, q_j) f_\gamma(q_j) w_j \\
f_\alpha(q_i) &- \sum_{j=1}^{N} K_{\alpha\beta}(E_3, q_i, q_j) f_\beta(q_j) w_j - \sum_{j=1}^{N} K_{\alpha\gamma}(E_3, q_i, q_j) f_\gamma(q_j) w_j = 0 \\
&\left( \delta_{ij} - \sum_{j=1}^{N} K_{\alpha\beta}(E_3, q_i, q_j) w_j - \sum_{j=1}^{N} K_{\alpha\gamma}(E_3, q_i, q_j) w_j \right) \begin{pmatrix} f_\alpha(q_i) \\ f_\beta(q_i) \\ f_\gamma(q_i) \end{pmatrix} = 0
\end{aligned} \tag{4.13}$$

where $\delta_{ij}$ is a Kronecker's delta, the dimension of the equation (4.13) depends on the number of mesh points. Then the matrix equation of the discretized kernel is a matrix by blocks

$$\begin{pmatrix} \mathbf{1} & H_{12} & H_{13} \\ H_{21} & \mathbf{1} & H_{23} \\ H_{31} & H_{32} & \mathbf{1} \end{pmatrix} \begin{pmatrix} f_a \\ f_b \\ f_c \end{pmatrix} = 0 \tag{4.14}$$

here $\mathbf{1}$ is the identity matrix. The matrix blocks ($H_{\alpha\beta}$) and $f_\alpha$ are given by

$$H_{\alpha\beta} = -\sum_{j=1}^{N} K_{\alpha\beta}(E_3, q_i, q_j) w_j \tag{4.15}$$

$$f_\alpha = f_\alpha(q_i) = \begin{pmatrix} f_\alpha(q_1) \\ f_\alpha(q_2) \\ \vdots \\ f_\alpha(q_N) \end{pmatrix} \tag{4.16}$$

where $0 \leq i \leq N$. We are able to write the elements of the matrix $H_{\alpha\beta}$ as

$$H_{\alpha\beta} = \begin{pmatrix} K_{\alpha\beta}(E_3, q_1, q_1) w_1 & K_{\alpha\beta}(E_3, q_1, q_2) w_2 & \cdots & K_{\alpha\beta}(E_3, q_1, q_N) w_N \\ K_{\alpha\beta}(E_3, q_2, q_1) w_1 & K_{\alpha\beta}(E_3, q_2, q_2) w_2 & \cdots & K_{\alpha\beta}(E_3, q_2, q_N) w_N \\ \vdots & \vdots & \ddots & \vdots \\ K_{\alpha\beta}(E_3, q_N, q_1) w_1 & K_{\alpha\beta}(E_3, q_N, q_2) w_2 & \cdots & K_{\alpha\beta}(E_3, q_N, q_N) w_N \end{pmatrix}. \tag{4.17}$$

As wee see, from equation (4.14) we have an equation of the type $HF = 0$, where $H$ and $F$ are matrices, this homogenous system will admit a non-trivial solution only if

$$\det H = \det \begin{pmatrix} \mathbf{1} & H_{12} & H_{13} \\ H_{21} & \mathbf{1} & H_{23} \\ H_{31} & H_{32} & \mathbf{1} \end{pmatrix} = 0 \tag{4.18}$$

the above determinant is a function of the three-body energy $E_3$, namely $h(E_3)$ and when the value $E_3$ correspond to a three-body bound state energy $E_3^n$ (the superscript $n$ labels the three-body energy for the $n^{th}$ bound state), the determinant of $H$ must be null

$$h(E_3^n) = 0 \tag{4.19}$$

then we have a function that only depends on the three-body bound state energy $E_3$. Choosing an interval of the energy $E_3$ and plotting against the function $h(E_3)$, we are able to see how this function behave and probably the closest values where the roots of this function are located (we may select two closest points $E_{3(0)}$ and $E_{3(1)}$). This will be helpful, because later we want to get the exact value of a root using the Secant-Method [46, 47], that it is an improvement of the Newton-Raphson method when we do not have access to the analytic expression of the function $h$ or its derivate $h'$.

Then by expanding the equation (4.19) up to the first order around $E_3$ we get

$$\begin{aligned} h(E_3^n) &= h(E_3) + (E_3^n - E_3)h'(E_3) = 0 \\ E_3^n &= E_3 - \frac{h(E_3)}{h'(E_3)}, \end{aligned} \tag{4.20}$$

where $h'(E_3) = \left.\frac{d\, h(E_3^n)}{dE_3^n}\right|_{E_3^n = E_3}$. Now from the definition of a derivate

$$h'(E_3) = \lim_{\Delta E_3 \to 0} \frac{h(E_3 + \Delta E_3) - h(E_3)}{\Delta E} \tag{4.21}$$

replacing the above definition into equation (4.20), and using a discrete notation for the energy (which means a new sub index $(m)$ )

$$E_3^n = E_{3(m-1)} - h(E_{3(m-1)}) \frac{E_{3(m-1)} - E_{3(m-2)}}{h(E_{3(m-1)}) - h(E_{3(m-2)})} \quad \text{for } m \geq 2 \tag{4.22}$$

here as we see, we need to guess two starting points ($E_{3(0)}$ and $E_{3(1)}$) as we discuss already. However we take advantage from a great propriety of the Kernel from equation (4.5 to 4.10) that presents the so-called well of attraction, which basically mean, even for bad guesses for the $E_3$, it would lead to the right final result.

## 4.2 Spectator Functions

Using the value already computed for the three-body bound-state energy $E_3^n$, it is necessary to replace once more into equation (4.14) in order to get the $H$ matrix. Now, our problem is to solve a set of 3N equations for 3N unknown variables, namely the spectator functions. However, the exact value of the three-body binding energy is the one which fulfills $\det H = 0$, meaning that one of the equations from the set of 3N variables is redundant and leading us to an underdetermined system. In other words, $3N - 1$ variables will be given in terms of an arbitrary value. Here we are setting $f_\alpha(q_1) = 1$, then the equation (4.14) become

$$\left( \begin{array}{|c|} \hline \\ \tilde{H}_{(3N-1)\times(3N-1)} \\ \\ \hline \end{array} \right)_{(3N\times 3N)} \begin{pmatrix} 1 \\ f_a(q_2) \\ \vdots \\ f_a(q_N) \\ f_b(q_{N+1}) \\ \vdots \\ f_b(q_{2N}) \\ f_c(q_{2N+1}) \\ \vdots \\ f_c(q_{3N}) \end{pmatrix}_{3N\times 1} = 0 \quad (4.23)$$

using the Gauss-Jordan elimination method we solve the set algebraic equation in terms of $f_\alpha(q_1) = 1$.

## 4.3 Numerical Results

In literature exists an extensive information about the energy spectrum of three-atoms in 2D [15, 16, 17, 18, 19, 20, 21, 22], but very few information about the structure of three-body systems. In the theory developed in this thesis, the energy spectrum of a three-body system is a crucial element for the study of the structure of those systems. Due to that, we calculated the energy spectrum of an asymmetric system AAB changing the mass asymmetry. Then, we calculated the different mean-square radii.

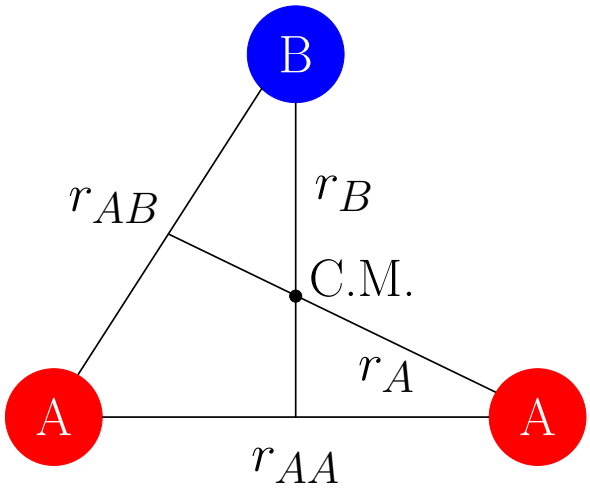


Figura 4.1: Schematic figure showing the three-body system of two equal particles, $A$, and one particle, $B$, allowed to differ. The point marked C.M. means center-of-mass of the three-body system. The notation used in this work for the relevant distances are also shown.

Figure 4.1, sketches an, AAB system, with two identical particles, A, and another distinguishable particle, B. Also the relevant distances to characterize this system are shown. The units that we use to obtain the numerical results obtained were $\hbar = m_A = E_{AA} = E_{AB} = 1$

### 4.3.1 Mass Dependence

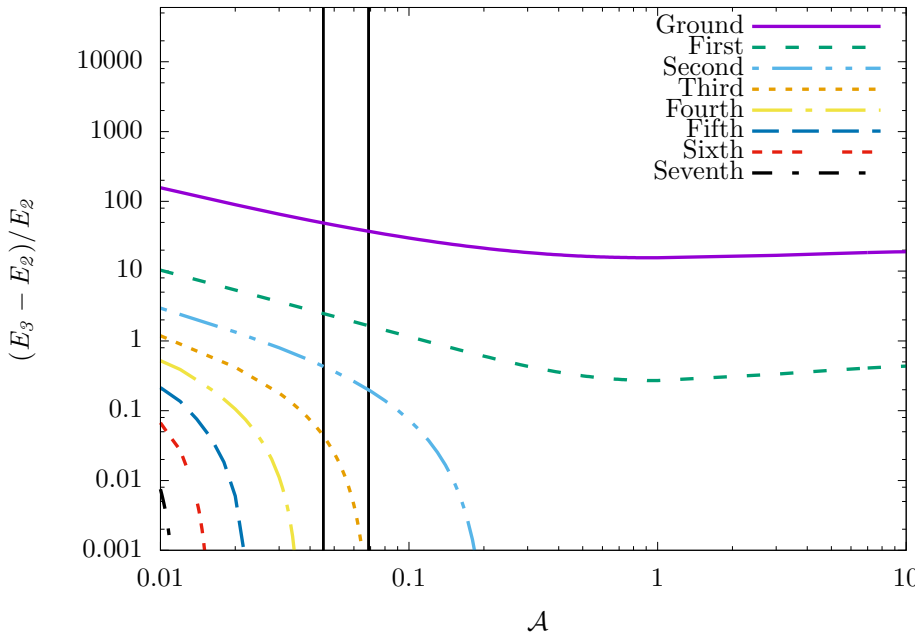


Figura 4.2: Low-energy spectrum of an $AAB$ system as a function of the mass ratio $\mathcal{A} = m_B/m_A$. The two two-body energies are equal, $E_{AB} = E_{AA} = E_2$, and the three-body energy is $E_3$. The energies on the $y$-axis are given relative to the two-body bound state energies, $E_2$. The vertical lines indicate the mass ratios $\mathcal{A} = 6/133$ and $\mathcal{A} = 6/87$ corresponding to the systems $^6$Li-$^{133}$Cs-$^{133}$Cs and $^6$Li-$^{87}$Rb-$^{87}$Rb. Only ground state and first excited states are bound for $\mathcal{A} \geq 1$.

In figure 4.2 we show the energy spectrum obtained from the numerical solution of the coupled integral Equations. (4.1). A similar figure can be found in [48] for other physical conditions.

There are many characteristic we can analyze from the energy spectrum result. One of them is the tremendously increase of the number of three-body bound states with decreasing mass ratio $\mathcal{A}$. In the figure 4.2 the smallest mass ratio we show is $\mathcal{A} = 0.01$ where the system displays eight bound states of energies $E_3$. As we start to increase the mass ratio, the excited three-body states disappear remaining only the first and ground states. For $\mathcal{A} = 1$, we recover the well known result, where only exist the ground and first excited states, bounded with energies $E_3 = 16.52E_2$ and $E_3 = 1.27E_2$. The dramatic mass dependence when decreasing $\mathcal{A}$ can be understood as a consequence of the increase of the effective interaction generated by the light particle. This has been known since 1978 for three dimensions [49] and since 1980 for two dimensions [50]. These derivations assumed the Born-Oppenheimer approximation, where the validity only is justified for $\mathcal{A} \ll 1$. In this scenario it is valid get an

effective hamiltonian for the relative motion of the two heavy particles dependents on the relative coordinate between them (R) as

$$H_{BO} = -\frac{\hbar^2}{2\mu_{AA}}\Delta_{\vec{R}_{AA}} + V_{AA}(R_{AA}) + V^{(BO)}(R_{AA}) \ , \tag{4.24}$$

where $\mu_{AA}$ is the reduced mass, $V_{AA}(R_{AA})$ is the two-body potential and $V^{(BO)}(R_{AA})$ is the strongly $\mathcal{A}$ depending Born-Oppenheimer potential resulting from the light particle B. By taking the expression from the literature of the $V^{(BO)}(R_{AA})$ found by [51] where it was derived analytically as a function of $\mathcal{A}$ in both limits of small and large distances and written in an asymptotic form as

$$V^{(BO)}(R) = -\frac{2e^{-\gamma}}{\sqrt{\frac{4m}{m+2}}R}\left(1 - \frac{e^{-\gamma}}{2}\sqrt{\frac{4m}{m+2}}R\left[(1-\gamma) - \frac{1}{2}\ln\left(\frac{e^{-\gamma}}{2}\sqrt{\frac{4m}{m+2}}R\right)\right]\right)^{-1} \tag{4.25}$$

for $\sqrt{\frac{4m}{m+2}}R \leq 1.15$

$$V^{(BO)}(R) = -1 - \sqrt{2\pi}\frac{e^{-\sqrt{\frac{4m}{m+2}}R}}{\sqrt{\left(\sqrt{\frac{4m}{m+2}}\right)^{\frac{1}{2}}R}} \tag{4.26}$$

for $\sqrt{\frac{4m}{m+2}}R \geq 1.15$. We may find more details in ref [51].

Now using small values for the mass ratio $\mathcal{A}$

$$m_{ef} = \left(\frac{4\mathcal{A}}{2+\mathcal{A}}\right)^{1/2} \approx \sqrt{2\mathcal{A}} \tag{4.27}$$

then the equations (4.26) and (4.27) for the limits of the effective potential in this approximation are

$$V^{(BO)}(R) \approx -\frac{2|E_{AB}|\exp(-\gamma)}{m_{ef}R} \quad \text{for} \quad m_{ef}R \leq 1.15 \ , \tag{4.28}$$

$$V^{(BO)}(R) \approx -|E_{AB}|\Big(1 + \frac{\sqrt{2\pi}\exp(-m_{ef}R)}{\sqrt{m_{ef}R}}\Big) \quad \text{for} \quad m_{ef}R \geq 1.15 \ , \tag{4.29}$$

where $\gamma = 0.5772156649$ is Euler's constant, and $R$ is the dimensionless measure of distance given in units of $(\hbar^2/m_A|E_{AA}|)^{1/2}$.

As we may see from equation (4.29) the large-distance behavior is an exponential approach towards the two-body energy with a length scale proportional to $1/m_{ef}$.

The small-distance behavior from equation 4.28 is located in the strong attractive region in the lowest energy states at small distance. It have a Coulomb-like attractive behavior with a charge of $2|E_{AB}|\exp(-\gamma)/m_{ef} \approx \sqrt{2/\mathcal{A}}|E_{AB}|\exp(-\gamma)$. In this

approximation we may say that our system become in hydrogen-like atom with a typical solution in three-dimension of the energy spectrum as

$$E_{\ell n_r} = -\left(\frac{e^2}{\hbar c}\right)\frac{mc^2}{2(\ell+1+n_r)^2} \tag{4.30}$$

with $n_r = 0, 1, 2, \cdots$ as the radial quantum number. Taking equation (4.30), using our units, the charge mentioned before and the mass ratio it lead us to

$$E^{(BO)}_{\ell n_r} = -\frac{\exp(-2\gamma)}{2\mathcal{A}(n_r+\ell+1)^2}\,, \tag{4.31}$$

this is a energy spectrum solution in the Born-Oppenheimer potential for a three-dimensional case. We are able to lead these solution into the two dimensional case for the hydrogen atom by setting $\ell = -1/2$ (we also may find more information of the two dimension energy spectrum of the hydrogen atom in the references [52, 53, 54]).

$$E^{(BO)}_{3} = -\frac{0.630473504}{\mathcal{A}(2n+1)^2}\,, \tag{4.32}$$

with $n = 0, 1, 2, \cdots$. Now we are in position to relate the energies displayed in figure 4.2 with the equation (4.32) but applied for $\mathcal{A} \ll 1$. We first notice that each state roughly follows the predicted linear decrease on the logarithmic scale for smalls $\mathcal{A}$. The calculated energies for a mass rate $\mathcal{A} = 0.01$ are almost reproduced by the Born-Oppenheimer estimates. Those conclusions hold as long as the Born-Oppenheimer approximation are valid and the states are located within the small distances of the Coulomb attraction.

| | $\mathcal{A}$ | $E_3^{(BO)}/E_{AB}$ | $E_3^{(NI)}/E_{AB}$ | $E_3/E_{AB}$ |
|---|---|---|---|---|
| Ground | 0.01 | 63.04 | 53.07 | 157.56 |
| | 0.02 | 31.52 | 27.76 | 90.75 |
| First | 0.01 | 7.00 | 7.72 | 11.34 |
| | 0.02 | 3.50 | 4.25 | 6.36 |
| Second | 0.01 | 2.52 | 3.21 | 3.94 |
| | 0.02 | 1.26 | 1.92 | 2.34 |
| Third | 0.01 | 1.28 | 1.92 | 2.18 |
| | 0.02 | 0.64 | 1.28 | 1.42 |

Table 4.1: Energies of ground and first excited states for the mass ratios $\mathcal{A} = 0.01$, 0.02 for the analytic Born-Oppenheimer approximation, $E_3^{(BO)}$ (in Eq. (4.32)), the numerical results both without, $E_3^{(NI)}$, and with, $E_3$, an interaction between the two heavy $A$-particles.

We can use Eq. (4.32) as a useful reference spectrum for comparison to the energies in the limit of $\mathcal{A} \ll 1$, shown in Fig. 4.2. To do this we have to distinguish between the present calculations and the pure Coulomb spectrum obtained

by neglecting the short-range potential between the two heavy $A$-particles. We compare these results in Table 4.1 for the lowest two bound states. The pure Born-Oppenheimer binding energies in the first column turn out to be larger by about 15 % for the two lowest states than the numerically calculated energies for precisely the same system. These deviations, already verified in Ref. [20], arise entirely from the inherent approximation in the Born-Oppenheimer procedure, that is neglect of recoil energy of the heavy particles. This difference has the same origin as the non-adiabatic diagonal term in an adiabatic expansion like in [14].
The numerical inaccuracy in these computations are much smaller and rather on the level of fractions of permille. It is probably useful here to emphasize that omission of the $AA$-interaction in the present two dimensions is completely equivalent to use of zero binding energy between the two $A$-particles. This is seen formally by letting $E_{AA}$ approach zero in Eqs.(4.2), (4.3) and (4.4).

We now present the background behavior through the different distances defined before in equations (3.23), (3.27), (3.31), (3.35), (3.36) and (3.37) of the three-body system showed in figure 4.1. There exist many facts we can analyze in order to test the results obtained are well behaved and expected. Anticipating before the graphics of the different radii we may suppose that at some point the radii from the second forward excited states are going to diverge as the figure 4.2 of the spectrum energy does.

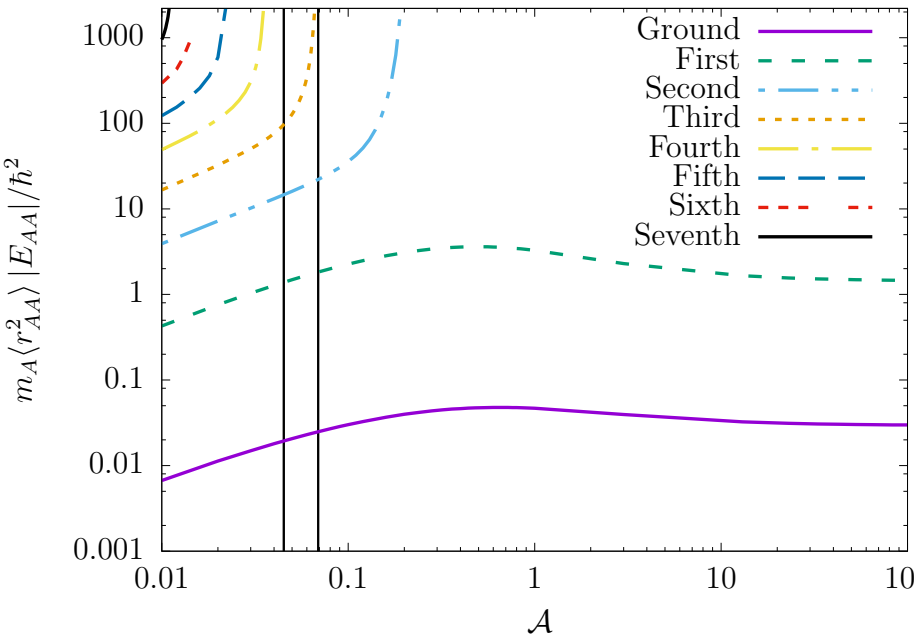


Figura 4.3: Dimensionless product $m_A\langle r_{AA}^2\rangle|E_{AA}|/\hbar^2$ ($E_{AA} = E_{AB}$) as a function of the mass ratio $\mathcal{A}$. As $\mathcal{A}$ is increased the radii diverge at the threshold where the excited states disappear. The remaining ground and first excited states assume a constant value as $\mathcal{A} \to \infty$. Vertical lines are the mass ratios corresponding to the systems $^6$Li-$^{133}$Cs-$^{133}$Cs and $^6$Li-$^{87}$Rb-$^{87}$Rb.

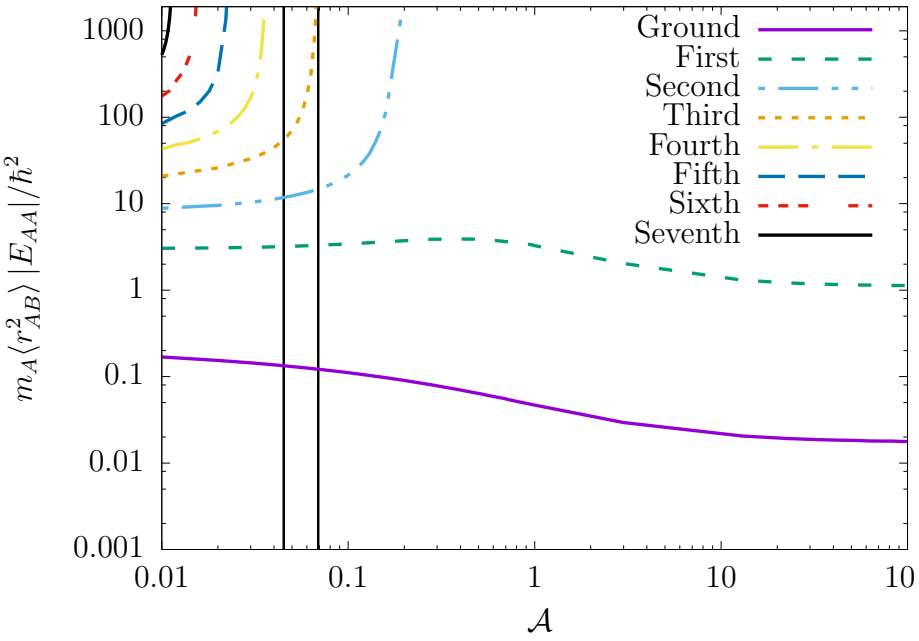


Figura 4.4: The same as Fig. 4.3 for $\langle r_{AB}^2 \rangle$.

At least one more distance is required to characterize the three-body geometric structure. We first choose the distance between unequal pairs of particles, $A$ and $B$. The mean-square radius is a quantum mechanical expectation value where the two identical particles cannot be distinguished. The results shown in Fig. 4.4 are therefore averages over distances between particle $B$ and the two $A$-particles. We notice first that the $AB$ mean-square distance is a flat or slightly increasing function with decreasing small mass ratios for both ground and first excited states. The higher-lying states show the opposite tendency of marginal decrease. Furthermore the $r_{AB}$-value in Fig. 4.4 is much larger than the $r_{AA}$ radius in Fig. 4.3, although with a difference decreasing with excitation energy. To understand this we cannot turn to the Born-Oppenheimer calculations which only provides information about the $AA$ system while the $B$-coordinate is integrated out. In the limit of small mass ratios the light $B$-particle is very little concerned with the slow relative $AA$ motion. The $B$-particle moves much faster and almost independently in an orbit of much larger radius.

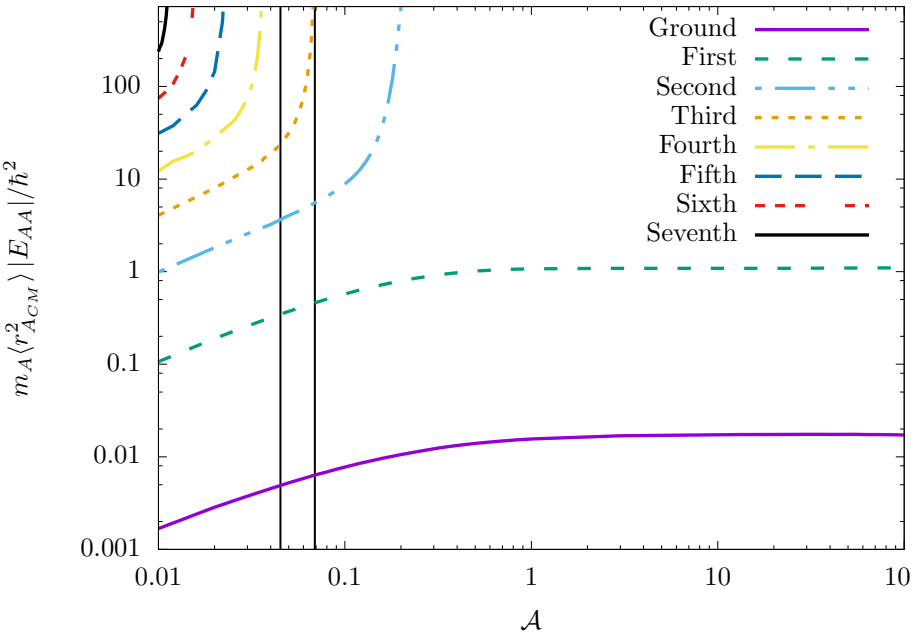


Figura 4.5: The same as Fig. 4.3 for $\langle r^2_{A_{CM}}\rangle$. As $\mathcal{A} \to \infty$ $\langle r^2_{A_{CM}}\rangle \to \langle r^2_{AB}\rangle$.

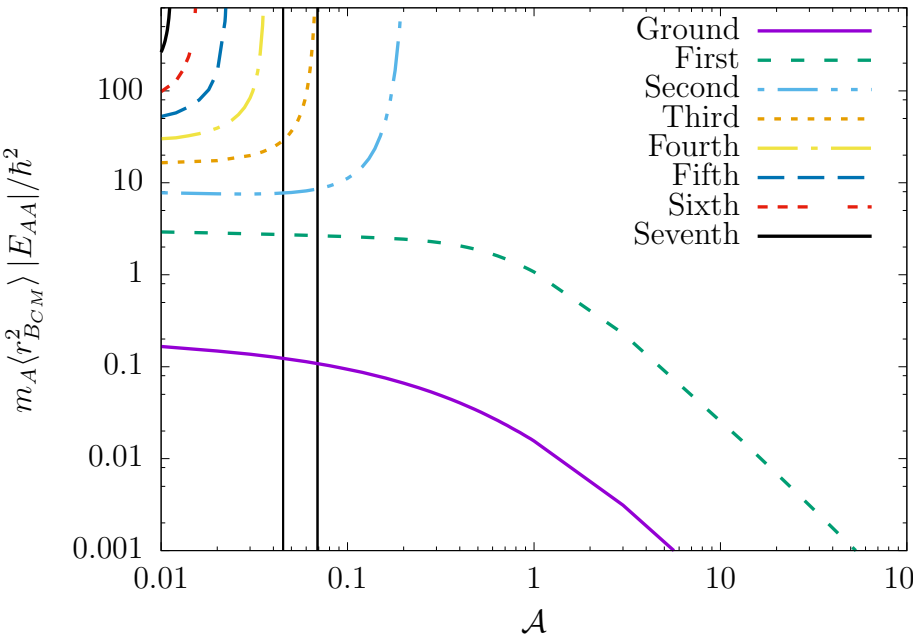


Figura 4.6: The same as Fig. 4.3 for $\langle r^2_{B_{CM}}\rangle$. As $\mathcal{A} \to \infty$ $\langle r^2_{B_{CM}}\rangle \to 0$.

Through the study and understanding of the energy spectrum as function of the mass ratio, we now want to analyze the corresponding results for the underlying structure. The figures 4.3, 4.5, 4.4 and 4.6 show the mean square distances $\langle r^2_{AA}\rangle$, $\langle r^2_A\rangle$, $\langle r^2_{AB}\rangle$ and $\langle r^2_B\rangle$, between the two identical particles $AA$, the center of mass of the system and the particle $A$, the particle $B$ and one of the identical particles $A$ and from the center of mass of the system and particle $B$, respectively.

From the radii figures, we may analyze some characteristics that lead us to believe in the consistence of the results. We may start by the symmetric case, where the masses of all particles are the same $\mathcal{A} = 1$, in this case we expect that the behavior of the system is similar to an equilateral triangle and the distances $\langle r^2_{AA}\rangle = \langle r^2_{AB}\rangle$ and $\langle r^2_A\rangle = \langle r^2_B\rangle$ follow those conditions. From the numerical calculations we obtain the next values, showed in table 4.2 and 4.3, for the ground and the first excited states

| $E_3/E_2$ | $\mathcal{A}$ | $\langle r^2_{AA}\rangle E_2$ | $\langle r^2_{AB}\rangle E_2$ | $\langle r^2_A\rangle E_2$ | $\langle r^2_B\rangle E_2$ |
|---|---|---|---|---|---|
| 16.5238 | 1 | 0.04678 | 0.04684 | 0.01558 | 0.01557 |

Table 4.2: Numerical results for ground state for the symmetric case where the mass ratio $\mathcal{A} = 1$. They follow the geometry of an equilateral triangle for the different mean square radial distances.

| $E_3/E_2$ | $\mathcal{A}$ | $\langle r^2_{AA}\rangle E_2$ | $\langle r^2_{AB}\rangle E_2$ | $\langle r^2_A\rangle E_2$ | $\langle r^2_B\rangle E_2$ |
|---|---|---|---|---|---|
| 1.2704 | 1 | 3.2737 | 3.2739 | 1.07307 | 1.07309 |

Table 4.3: Numerical results in first excited state for the symmetric case where the mass ratio $\mathcal{A} = 1$. They follow the geometry of an equilateral triangle for the different mean square radial distances.

Another important result is when $\mathcal{A} \to \infty$, at this point the center of mass of the system is dislocated towards direction of the particle B and the distances $\langle r^2_B\rangle \to 0$ and $\langle r^2_A\rangle \to \langle r^2_{AB}\rangle$ follow those conditions. From the numerical calculations we obtain the next values, showed in table 4.4 and 4.5, for the ground and the first excited state

| $E_3/E_2$ | $\mathcal{A}$ | $\langle r^2_{AA}\rangle E_2$ | $\langle r^2_{AB}\rangle E_2$ | $\langle r^2_A\rangle E_2$ | $\langle r^2_B\rangle E_2$ |
|---|---|---|---|---|---|
| 21.6023 | $10^2$ | 0.02986 | 0.01777 | 0.01724 | $4.675 * 10^{-6}$ |

Table 4.4: Numerical results in ground state for $\mathcal{A} \to \infty$ case. They follow those condition: $\langle r^2_B\rangle \to 0$ and $\langle r^2_A\rangle \to \langle r^2_{AB}\rangle$.

| $E_3/E_2$ | $\mathcal{A}$ | $\langle r^2_{AA}\rangle E_2$ | $\langle r^2_{AB}\rangle E_2$ | $\langle r^2_{A}\rangle E_2$ | $\langle r^2_{B}\rangle E_2$ |
|---|---|---|---|---|---|
| 1.51119 | $10^2$ | 1.461589 | 1.13088 | 1.10259 | $2.9237 * 10^{-4}$ |

Table 4.5: Numerical results in first excited state for $\mathcal{A} \to \infty$ case. They follow those condition: $\langle r^2_B\rangle \to 0$ and $\langle r^2_A\rangle \to \langle r^2_{AB}\rangle$.

When $\mathcal{A} \to 0$ the center of mass of the system is going to be close to the particles $AA$ and that implies that $r_A$ is going to approach to $r_{AA}/2$. This means that the different mean square radii are going to follow the condition $\langle r^2_A\rangle \to \langle r^2_{AA}\rangle/4$, as can be seen in tables 4.6 and 4.7.

| $E_3/E_2$ | $\mathcal{A}$ | $\langle r^2_{AA}\rangle E_2$ | $\langle r^2_{AB}\rangle E_2$ | $\langle r^2_{A}\rangle E_2$ | $\langle r^2_{B}\rangle E_2$ |
|---|---|---|---|---|---|
| 157.5634 | $10^{-2}$ | 0.006702 | 0.16888 | 0.001675 | 0.16577 |

Table 4.6: Numerical results in ground state for $\mathcal{A} \to 0$ case. They follow those condition: $\langle r^2_A\rangle \to \langle r^2_{AA}\rangle/4$.

| $E_3/E_2$ | $\mathcal{A}$ | $\langle r^2_{AA}\rangle E_2$ | $\langle r^2_{AB}\rangle E_2$ | $\langle r^2_{A}\rangle E_2$ | $\langle r^2_{B}\rangle E_2$ |
|---|---|---|---|---|---|
| 11.34824 | $10^{-2}$ | 0.427928 | 3.05216 | 0.106568 | 2.92115 |

Table 4.7: Numerical results in first excited state for $\mathcal{A} \to 0$ case. They follow those condition: $\langle r^2_A\rangle \to \langle r^2_{AA}\rangle/4$.

There are another kind of considerations that we can analyze from the behavior of the Figures 4.3, 4.5, 4.4 and 4.6 of the mean square distances. When $\mathcal{A} \to 0$, the center of mass of the system will dislocate towards the two particles $AA$ and the distance from the center of mass and the particle $B$ is going to increase. That is exactly what we see from figure 4.6 for the ground and first state. At the same time the distance from the center of mass and the particle $A$ is going to decrease as the figure 4.5 shows it.

By the Born-Oppenheimer approximation we directly relate the radii for small mass ratios with a Coulomb orbits because for small mass ratios we may say we have a Coulomb-like attractive potential, see equation (4.28). Then the values for the $\langle r^2_{AA}\rangle$ are given analytically by

$$< r^2_{AA} >= \mathcal{A}\exp(2\gamma)(n_r+\ell+1)^2\Big(5(n_r+\ell+1)^2+1-3\ell(\ell+1)\Big)\,, \tag{4.33}$$

with $n_r = 0, 1, 2, \cdots$, remembering that this equation is for the three dimensional case. By setting $\ell = -1/2$ we goes to the two dimensional case

$$< r^2_{AA} >= \frac{3.1722}{16}\mathcal{A}(2n+1)^2(5(2n+1)^2+7)\,, \tag{4.34}$$

where we again have that $n = 0, 1, 2, \cdots$, which only is valid for sufficiently small $\mathcal{A}$. Figure 4.3 qualitatively reproduces the Born-Oppenheimer estimate from equation (4.34).

| | $\mathcal{A}$ | $\langle r_{AA}^{(BO)2} \rangle / R_u^2$ | $\langle r_{AA}^{(NI)2} \rangle / R_u^2$ | $\langle r_{AA}^2 \rangle / R_u^2$ |
|---|---|---|---|---|
| Ground | 0.01 | 0.023 | 0.029 | 0.006 |
| | 0.02 | 0.047 | 0.056 | 0.011 |
| First | 0.01 | 0.923 | 0.916 | 0.427 |
| | 0.02 | 1.837 | 1.767 | 0.757 |
| Second | 0.01 | 6.510 | 6.268 | 3.911 |
| | 0.02 | 12.955 | 12.254 | 7.201 |
| Third | 0.01 | 24.359 | 23.381 | 16.594 |
| | 0.02 | 48.478 | 48.534 | 32.219 |

Table 4.8: Mean-square-radii in the Born-Oppenheimer approximation, $\langle r_{AA}^{(BO)2} \rangle$, from Eq. (4.34), and numerical results without, $\langle r_{AA}^{(NI)2} \rangle$, and with, $\langle r_{AA}^2 \rangle$, the interaction between the two $A$-particles. All these lenghts are in units of $R_u \equiv \hbar / \sqrt{m_A |E_{AB}|}$.

Let us first consider the radii of the states obtained for the smallest mass ratios of $\mathcal{A} = 0.01$, 0.02. We compare with the Born-Oppenheimer estimates precisely as we did for the energies in Table 4.8. We observe the opposite behavior compared to the energies, that is the mean square radii are largest for the smallest binding energies. The results for the two lowest states for rigorous Born-Oppenheimer are about 15 % smaller than obtained from the full numerical calculation without an $AA$ interaction. These deviations are again due to the neglect of recoil energy as assumed in the Born-Oppenheimer prescription. The observed opposite tendency is reflected in the formula in Eqs. (4.32) and (4.34) where the product is state independent apart from the last factor in Eq. (4.34).

We now turn to the full calculation with sizable two-body energies between all three pairs of particles, shown in the last column of Table 4.8. The ground state mean-square radius is a factor of about 3.5 smaller than derived from the Coulomb estimate in Eq. (4.34). This deviation is again qualitatively consistent with the similar larger binding energy of that state. The first excited state is only smaller than the Coulomb estimate by a factor of 2.2. The following two higher-lying states have radii rather similar to the Coulomb estimates. These states extend beyond the Coulomb region and into the region of the more confining large-distance Born-Oppenheimer potential from Eq. (4.28). The effect is a comparably smaller spatial extension which is very close to the results from Eq. (4.34).

In order to investigate in more details how the structure varies when the energy of a state approaches its threshold for binding, we will to use the second excited state

which is the lowest excited state that disappears at the threshold. By multiplying the radii for a linear function of the energy above the threshold, $E_3 - E_2$, we obtain the behavior of the divergence. Figure 4.7 shows the divergence of the different mean square radii for the second excited state.

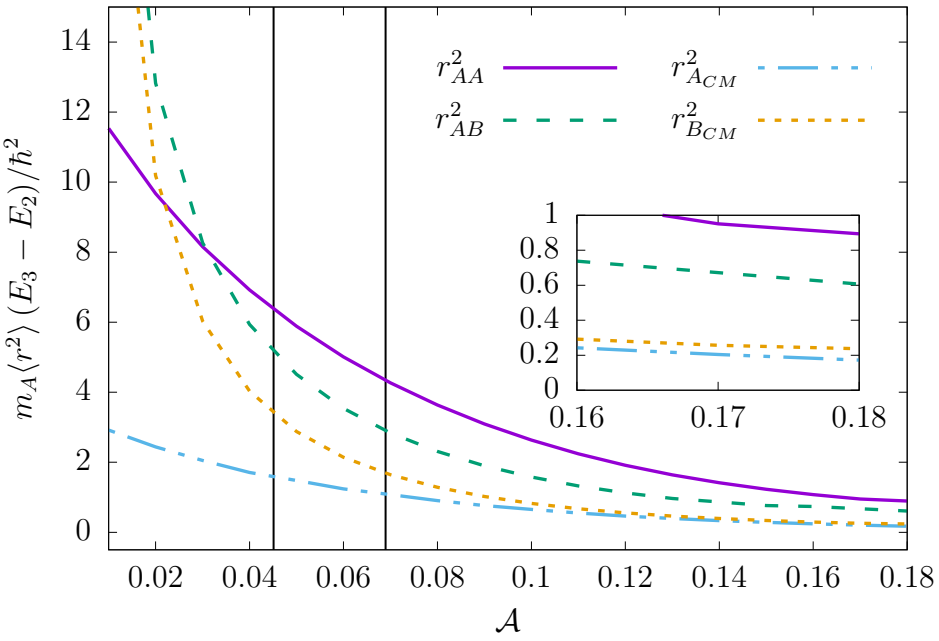


Figura 4.7: The threshold behavior of different mean-square radii for the second excited state as function of mass ratio. The divergent mean-square radii reach a constant value at threshold when multiplied by $E_3 - E_2$. Vertical lines are the mass ratios corresponding to the systems $^6$Li-$^{133}$Cs-$^{133}$Cs and $^6$Li-$^{87}$Rb-$^{87}$Rb.

The striking results are the constant values for the product $\langle r^2\rangle(E_3 - E_2)$ as the threshold is approached. Because the divergence is proportional to $E_3 - E_2$, this implies that the threshold structure must have the energy, $E_3 - E_2$, corresponding to one bound two-body system. Two structures seems to be intuitively possible at threshold, that is either particle $A$ or particle $B$ is ejected while the remaining pair settles in their ground state, as we show in figures (4.8 and 4.9). In both cases the threshold structure resembles two-body systems, that is $(AA) - B$ or $(AB) - A$ with corresponding reduced masses $\mu_{AA,B} \approx 0.18$ for the case shown in figure (4.8) and $\mu_{AB,A} \approx 0.54$, for the case shown in figure (4.9) where we used a threshold value of $\mathcal{A} \approx 0.2$.

These structures would according to ref. [25] lead to the two-body divergences, $< r^2_{ij} >= \hbar^2/(3\mu_{ij,k}|E_{th}|)$, where $\mu_{ij,k}$ and $|E_{th}|$ are three-body reduced mass and the vanishing threshold energy, respectively, the $i, j, k$ indices follow a cyclical permutation of the particles (AAB). By using our natural units, the divergence near to the threshold value will follow the relation

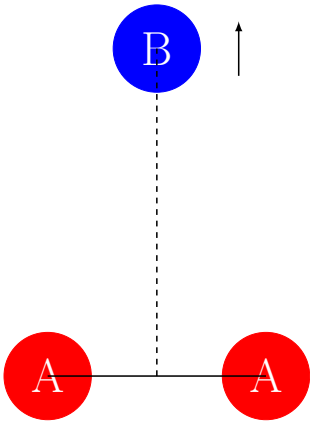


Figura 4.8: Threshold structure. In this case the particles AA remain bounded and the particle B is ejected.

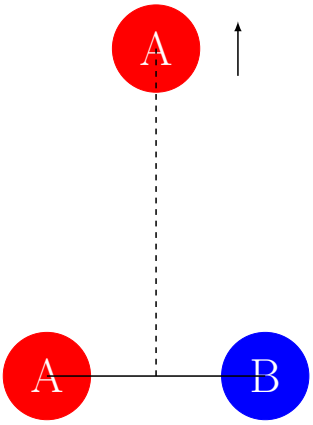


Figura 4.9: Threshold structure. In this case the particles AB remain bounded and the particle A is ejected.

$$< r_{ij}^2 > |E_{th}| = \frac{1}{3\mu_{ij,k}} \tag{4.35}$$

This means that for the first case, figure (4.8) where the particles AA are bound the particle B is ejected, the divergence behavior for the quantity is expected to be $< r_{AA}^2 > |E_{th}|/\hbar^2 \to 0$ due to the fact that threshold energy tends to zero while the mean square radius for the bound particles AA is finite and $< r_{AB}^2 > |E_{th}|/\hbar^2 \to 1.85$ due to the mean square radius for the particle B goes to infinity. For the second case, figure (4.9) both mean square radii are growing, and the divergence behavior is $< r_{AA}^2 > |E_{th}|/\hbar^2 \to 0.62$ and $< r_{AB}^2 > |E_{th}|/\hbar^2 \to 0.62$.

If we compare these results obtained for the two cases discussed above with the result obtained in the figure (4.7), the best match is the second case, where one of the A-particles is ejected. In the calculated expectation value is contained an average over the distances between the two $A$-particles and particle $B$. One of these distances remains finite and do not contribute except through a reduction of the probability by a factor of 2. This accounts for the value of $\frac{m_A < r_{AB}^2 >}{\hbar^2}(E_3 - E_2) = 0.6$, being only about two thirds of $\frac{m_A < r_{AA}^2 >}{\hbar^2}(E_3 - E_2) = 0.9$, at threshold.

# Chapter 5

# Conclusions

In this thesis we developed the equations for the structure of a three-body system formed by using a two-body Dirac-$\delta$ potential in momentum space in two dimensions. We saw that for short-range potentials the observables of a three-body system can be represented as a universal scale function. This independence on the form of the potential is valid only when the two-body scattering length is much greater than the range of the potential. We computed all distances to characterize our three-body system for a mass ratio supporting up to eight bound states. The development of our formalism in momentum space may be suitable to study such weakly-bound systems as in configuration space the tail of the three-body wave function should extend considerably making the numerical part of the calculation more difficult. The mean square radii were extracted here from the derivative of the one and two-body form factors, which is also easier than to perform the complete Fourier transform of the wave function.

The technique used here may be easily extended to a fully asymmetric system considering even unbound two-body subsystems. Our zero-range calculation, which is the limit for the short-range potentials, provides a qualitative guide for the experimentalists to study the universal behavior of the structure of molecules inside a mixed species atomic trap.

For the system we studied (AAB), the relevant parameters were the two-body energies and the mass ratios. For our purposes we considered equal two-body energies and varied the mass ratio. We saw a very different behavior for small and large mass ratios. For the energy spectrum we obtained the same result as previous calculations: as the mass ratio is decreased the number of three-body bound states increases. As this mass ratio is increased only the ground and first excited state survive. Small mass ratio was analyzed through the Born-Oppenheimer approximation of the potential. The effective interaction generated by the light particle has a Coulomb like behavior for small distances between particles of the heavier pair. This is the most attractive region and consequently where the lowest states are located. Considering this Coulomb potential, the three-body energies and A-A radii were derived and compared to the full calculations. We saw a qualitative very good agreement. The quantitative agreement should be checked for different two-body

energies in such a way the distance between the heavy particles can be made small comparing to the other distances.

We discussed the different radii results for the limits of small and large mass ratios, where some distances should match. The radii close to the mass ratio threshold diverge proportional to the three-body energy measured with respect to the two-body threshold. The analysis of the different radii permitted to conclude that at the threshold we have a bound AB pair and the ejection of particle A. In the figures we showed explicitly the mass ratios for the recent set of atoms $^{6}$Li-$^{133}$Cs-$^{133}$Cs and $^{6}$Li-$^{87}$Rb-$^{87}$Rb produced experimentally.

In summary, the present work contribute to the characterization of the many variations of universal three-body structures in two dimensions. We confined ourselves to two-body mean square moments in AAB systems where each pair is bound with the same energy.

For future works we are planing to vary the ratio of two-body energies and extract mean square radii when thresholds of two-body binding are approached. Also extensions into the two-body continuum, still for bound three-body systems, would be another set of interesting investigations. The last tempting generalization is the ABC systems with three different particles.

# Appendix A

# The $S$ matrix

The collision matrix or collision operator which relates the state vectors describing the system in the remote past ($t' \to -\infty$) and in the far future ($t \to +\infty$) is defined as

$$S \equiv U(+\infty, 0)U(0, -\infty) = \Omega^{(-)\dagger}\Omega^{(+)} \tag{A.1}$$

where $\Omega^{(\pm)}$ are the Møller operators [38]. We assume that his operator acts on the eigenstates $\Phi_\alpha$ and $\Phi_\beta$ two asymptotic free states of $H_0$. The matrix elements of this operator $S$ between this two states are

$$\langle\Phi_\beta|S|\Phi_\alpha\rangle = \langle|\Phi_\beta|\Omega^{(-)\dagger}\Omega^{(+)}|\Phi_\alpha\rangle = \langle\Psi_\beta^{(-)}|\Psi_\alpha^{(+)}\rangle \tag{A.2}$$

where we have used $|\Psi_\alpha^{(\pm)}\rangle = \Omega^{(\pm)}|\Phi_\alpha\rangle$. We also note that the elements are time-independent.

## A.1 Properties of the collision operator

The collision operator is unitary

$$\begin{aligned} S^\dagger S &= \Omega^{(+)\dagger}\Omega^{(-)}\Omega^{(-)\dagger}\Omega^{(+)} \\ &= \Omega^{(+)\dagger}(I - \Lambda)\Omega^{(+)} \\ &= \Omega^{(+)\dagger}\Omega^{(+)} - \Omega^{(+)\dagger}\Lambda\Omega^{(+)} \\ &= I \end{aligned} \tag{A.3}$$

where we use that $\sum \Omega^{(\pm)}\Omega^{(\pm)\dagger} = I - \Lambda$ and $\Lambda = |\Psi^{(B)}\rangle\langle\Psi^{(B)}|$ represent the bound states of the system. Remembering that the Møller operator annihilate the bound state $\Omega^{(+)\dagger}\Lambda = 0$ [38].

Another important propriety that the collision operator inherited from the Møller operators $H\Omega^{(\pm)} = \Omega^{(\pm)}H_0$, is that

$$\begin{aligned} \Omega^{(-)\dagger}H\Omega^{(+)} &= \Omega^{(-)\dagger}\Omega^{(+)}H_0 \\ \Omega^{(-)\dagger}H\Omega^{(+)} &= H_0\Omega^{(-)\dagger}\Omega^{(+)} \end{aligned} \tag{A.4}$$

therefore

$$[S, H_0] = 0 \tag{A.5}$$

## A.2 Relation between Collision Operator $S$ and Transition Operator $T$

From equation (A.2) we add and subtract $\langle\Psi_b^{(+)}|$ to be rewritten as

$$\begin{aligned}\langle\Phi_\beta|S|\Phi_\alpha\rangle &= \langle\Psi_\beta^{(+)}|\Psi_\alpha^{(+)}\rangle + \langle\Psi_\beta^{(-)} - \Psi_\beta^{(+)}|\Psi_\alpha^{(+)}\rangle \\ &= \delta_{\alpha\beta} + \langle\Psi_\beta^{(-)} - \Psi_\beta^{(+)}|\Psi_\alpha^{(+)}\rangle \end{aligned} \tag{A.6}$$

and using the hermicity of $H$ and $V$ and the explicit form of the Møller operator[38], we may write $\langle\Psi_\beta^{(\pm)}| = \langle\Phi_\beta| + \lim_{\epsilon\to 0^+}\langle\Phi_\beta|\frac{V}{E_\beta - H \mp i\epsilon}$. In this way, the equation (A.6) is rewrite as

$$\begin{aligned}\langle\Phi_\beta|S|\Phi_\alpha\rangle &= \delta_{\alpha\beta} + \lim_{\epsilon\to 0^+}\langle\Phi_\beta|\frac{V}{E_\alpha - H + i\epsilon} - \frac{V}{E_\beta - H - i\epsilon}|\Psi_\alpha^{(+)}\rangle \\ &= \delta_{\alpha\beta} + \lim_{\epsilon\to 0^+}\left(\frac{1}{E_\beta - E_\alpha + i\epsilon} - \frac{1}{E_\beta - E_\alpha - i\epsilon}\right)\langle\Phi_\beta|V|\Psi_\alpha^{(+)}\rangle \\ &= \delta_{\alpha\beta} - \lim_{\epsilon\to 0^+}\frac{2i\epsilon}{(E_\beta - E_\alpha)^2 + \epsilon^2}\langle\Phi_\beta|V|\Psi_\alpha^{(+)}\rangle. \end{aligned} \tag{A.7}$$

Now we consider the limit expression, we have two cases: The first case is if $E_\alpha \neq E_\beta$ then the limit will vanish. The second case If $E_\alpha = E_\beta$ then the limit get an infinity value. As we see the behavior of that limits is similar to a delta function for the energies $E_\alpha$ and $E_\beta$ then we may write

$$\pi\delta(E_\alpha - E_\beta) = \lim_{\epsilon\to 0^+}\frac{\epsilon}{(E_\beta - E_\alpha)^2 + \epsilon^2} \tag{A.8}$$

the constraint $\pi$ is due to the fact that the integral of this function over the all spectra values of the Energies must be equal to 1, we easily can prove this by performing the integral $\int_{E_0}^{\infty}\lim_{\epsilon\to 0^+}\frac{\epsilon}{(E_\beta - E_\alpha)^2+\epsilon^2}dE_b$. Replacing the value of the limit (A.8) in our equation (A.7)

$$\langle\Phi_\beta|S|\Phi_\alpha\rangle = \delta_{\alpha\beta} - 2\pi i\delta(E_\beta - E_\alpha)\langle\Phi_\beta|V|\Psi_\alpha^{(+)}\rangle \tag{A.9}$$

through this equation (A.9) we do the connection with the transition operator, by using the equation (2.22) replacing into equation (2.19) and using the Dirac's notations

$$\begin{aligned}
\langle\Phi_\beta|S|\Phi_\alpha\rangle &= \delta_{\alpha\beta} - 2\pi i\delta(E_\beta - E_\alpha)\langle\Phi_\beta|V\left\{|\phi_\alpha\rangle + G^+V|\phi_\alpha\rangle\right\} && \text{(A.10)}\\
&= \delta_{\alpha\beta} - 2\pi i\delta(E_\beta - E_\alpha)\langle\Phi_\beta|\left\{V + VG^+V\right\}|\phi_\alpha\rangle && \text{(A.11)}\\
& && \text{(A.12)}
\end{aligned}$$

and from the definition of the transition operator, equation (2.1) we finally get

$$\langle\Phi_\beta|S|\Phi_\alpha\rangle = \delta_{\alpha\beta} - 2\pi i\delta(E_\beta - E_\alpha)\langle\Phi_\beta|T|\Phi_\alpha\rangle \qquad \text{(A.13)}$$

that is the relation between to important operators in the scattering theory, because they are highly related with the observables measured from collision experiments.

# Appendix B

# Jacobi Relative Momentum (Three-body System)

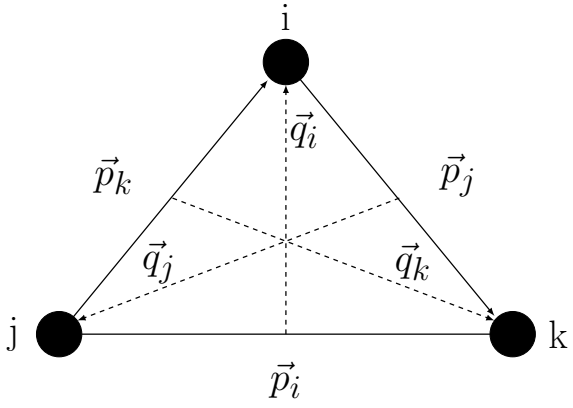


Figura B.1: The Jacobi coordinates.

If $\vec{k}_i + \vec{k}_j + \vec{k}_k = 0$ are the momentum of the particles in relation to the center of mass (C.M.); $m_\alpha$ and $v_\alpha$ with $(\alpha = i, j, k)$ are the masses and the velocities respectively. Then the Jacobi relative momentum are given by

$$\vec{p}_i = \frac{m_j m_k}{m_j + m_k}(\vec{v}_j - \vec{v}_k) = \frac{m_k \vec{k}_j - m_j \vec{k}_k}{m_j + m_k}, \tag{B.1}$$

and for the momentum $\vec{q}_\alpha$

$$\vec{q}_i = \frac{m_i(m_j + m_k)}{m_i + m_j + m_k}\left[\vec{v}_i - \frac{m_j \vec{v}_j + m_k \vec{v}_k}{m_j + m_k}\right] = \vec{k}_i \tag{B.2}$$

analogous we write $\vec{q}_j = \vec{k}_j$ and $\vec{q}_k = \vec{k}_k$. Then by linking the coordinates we obtain

$$\vec{p}_i = \frac{m_k \vec{q}_j - m_j \vec{q}_k}{m_j + m_k} \tag{B.3}$$

$$\vec{p}_j = \frac{m_i \vec{q}_k - m_k \vec{q}_i}{m_i + m_k} \tag{B.4}$$

$$\vec{p}_k = \frac{m_j \vec{q}_i - m_i \vec{q}_j}{m_i + m_j}. \tag{B.5}$$

# Appendix C

# Matrix Elements of the Free Green function in Momentum Space

The six matrix elements that appears in the equations (2.93, 2.94 and 2.95) are calculated for the different Jacobi relative momentum basis $\vec{p}_\alpha$ and $\vec{q}_\alpha$ with $\alpha = i, j, k$ (we will use $ME$ as the name of the Matrix Elements)

$$ME = \langle \chi_\alpha, \vec{q}_\alpha | \left( G_0^{(+)}(E_3) \right) | \chi_\beta \rangle | f_\beta \rangle \tag{C.1}$$

using the completeness relation as

$$\hat{1} = \int d^2 q_\beta |\vec{q}_\beta\rangle\langle\vec{q}_\beta| \tag{C.2}$$

$$\hat{1} = \int d^2 p_\alpha |\vec{p}_\alpha\rangle\langle\vec{p}_\alpha| \tag{C.3}$$

the equation (C.1) after setting the completeness relation is

$$\begin{aligned} ME \quad &= \int d^2 q_\beta \langle \chi_\alpha, \vec{q}_\alpha | \left( G_0^{(+)}(E_3) \right) | \vec{q}_\beta \rangle \langle \vec{q}_\beta | \chi_\beta \rangle | f_\beta \rangle \\ &= \int d^2 q_\beta d^2 p_\alpha d^2 p_\beta \langle \chi_\alpha, \vec{q}_\alpha | \vec{p}_\alpha \rangle \langle \vec{p}_\alpha | \left( G_0^{(+)}(E_3) \right) | \vec{p}_\beta \rangle \langle \vec{p}_\beta | \chi_\beta, \vec{q}_\beta \rangle f_\beta(\vec{q}_\beta) \\ &= \int d^2 q_\beta d^2 p_\alpha d^2 p_\beta \frac{g_\alpha(\vec{p}_\alpha) g_\beta(\vec{p}_\beta)}{E - \frac{\vec{q}_\alpha^2}{2m_{\beta\gamma,\alpha}} - \frac{\vec{p}_\alpha^2}{2m_{\beta\gamma}}} \langle \vec{q}_\alpha, \vec{p}_\alpha | \vec{p}_\beta, \vec{q}_\beta \rangle f_\beta(\vec{q}_\beta) \end{aligned} \tag{C.4}$$

and now we must calculate the elements $\langle \vec{q}_\alpha, \vec{p}_\alpha | \vec{p}_\beta, \vec{q}_\beta \rangle$ [45].

$$\langle \vec{q}_\alpha, \vec{p}_\alpha | \vec{p}_\beta, \vec{q}_\beta \rangle = \delta \left( \vec{p}_\alpha - \vec{p'}_\alpha(\vec{p}_\beta, \vec{q}_\beta) \right) \delta \left( \vec{q}_\alpha - \vec{q'}_\alpha(\vec{p}_\beta, \vec{q}_\beta) \right). \tag{C.5}$$

From the Jacobi relative momentum we may get the relations between different relative momentum, then from equations (B.3, B.4 and B.5) we may write

$$\vec{p'}_\alpha(\vec{p}_\beta, \vec{q}_\beta) = \quad \frac{m_\gamma \vec{q}_\beta - m_\beta \vec{q}_\gamma}{m_\beta + m_\gamma} \tag{C.6}$$

$$= \quad \frac{m_\gamma}{m_\beta + m_\gamma}\vec{q}_\beta - \frac{m_\beta}{m_\beta + m_\gamma}(-\vec{q}_\alpha - \vec{q}_\beta) \tag{C.7}$$

$$= \quad \vec{q}_\beta + \frac{m_\beta}{m_\beta + m_\gamma}\vec{q}_\alpha \tag{C.8}$$

and the first delta on the right-hand-side from the equation (C.5) is

$$\delta\left(\vec{p}_\alpha - \vec{p'}_\alpha(\vec{p}_\beta, \vec{q}_\beta)\right) = \delta\left(\vec{p}_\alpha - \vec{q}_\beta - \frac{m_\beta}{m_\beta + m_\gamma}\vec{q}_\alpha\right). \tag{C.9}$$

We too can find the relation which arrive from the momentum $\vec{q'}_\alpha$

$$\vec{q'}_\alpha(\vec{p}_\beta, \vec{q}_\beta) = \quad \frac{m_\gamma + m_\alpha}{m_\gamma}\vec{p}_\beta + \frac{m_\alpha}{m_\gamma}\vec{q}_\gamma \tag{C.10}$$

$$= \quad \frac{m_\gamma + m_\alpha}{m_\gamma}\vec{p}_\beta + \frac{m_\alpha}{m_\gamma}(-\vec{q}_\alpha - \vec{q}_\beta) \tag{C.11}$$

and replacing this relation founded above into the second delta term on the equation (C.5), we get

$$\delta\left(\vec{q}_\alpha - \vec{q'}_\alpha(\vec{p}_\beta, \vec{q}_\beta)\right) = \delta\left(\vec{p}_\beta + \vec{q}_\alpha + \frac{m_\alpha}{m_\gamma + m_\alpha}\vec{q}_\beta\right) \tag{C.12}$$

and remembering that for a $\delta$-Dirac's potential the form factor is $g(\vec{p}) = 1$. Replacing the values from the delta functions into equation (C.4)

$$ME = \quad \int d^2q_\beta d^2p_\alpha d^2p_\beta \frac{\delta\left(\vec{p}_\alpha - \vec{q}_\beta - \frac{m_\beta}{m_\beta+m_\gamma}\vec{q}_\alpha\right)\delta\left(\vec{p}_\beta + \vec{q}_\alpha + \frac{m_\alpha}{m_\gamma+m_\alpha}\vec{q}_\beta\right)}{E - \frac{\vec{q}_\alpha^2}{2m_{\beta\gamma,\alpha}} - \frac{\vec{p}_\alpha^2}{2m_{\beta\gamma}}} f_\beta(\vec{q}_\beta)$$

$$= \quad \int d^2q_\beta d^2p_\alpha d^2p_\beta \frac{f_\beta(\vec{q}_\beta)}{E - \frac{\vec{q}_\alpha^2}{2m_{\beta\gamma,\alpha}} - \frac{\left(\vec{q}_\beta + \frac{m_\beta}{m_\beta+m_\gamma}\vec{q}_\alpha\right)_\alpha^2}{2m_{\beta\gamma}}} \tag{C.13}$$

where finally we write the matrix elements (C.1) are given by

$$\langle\chi_\alpha, \vec{q}_\alpha|\left(G_0^{(+)}(E_3)\right)|\chi_\beta\rangle|f_\beta\rangle = \int d^2q_\beta d^2p_\alpha d^2p_\beta \frac{f_\beta(\vec{q}_\beta)}{E - \frac{q_\alpha^2}{2m_{\alpha\gamma}} - \frac{q_\beta^2}{2m_{\beta\gamma}} - \frac{1}{m_\gamma}\vec{q}_\beta.\vec{q}_\alpha}. \tag{C.14}$$

# Appendix D

# The Shifted Momenta

## D.1 The shifted momenta between particles B and C

The shifted momenta and the Hamiltonian can be written as

- $\left|\vec{p}+\frac{\vec{Q}}{2}-\frac{\mathcal{A}}{\mathcal{A}+1}\vec{q}\right| = \left(p^2+\frac{Q^2}{4}+\left(\frac{\mathcal{A}}{\mathcal{A}+1}\right)^2 q^2+pQ\cos(\theta_p)-2\frac{\mathcal{A}}{\mathcal{A}+1}pq\cos\left(\theta_q-\theta_p\right)-\frac{\mathcal{A}}{\mathcal{A}+1}Qq\cos\left(\theta_q\right)\right)^{1/2}$
- $\left|\vec{p}+\frac{\vec{Q}}{2}+\frac{1}{\mathcal{A}+1}\vec{q}\right| = \left(p^2+\frac{Q^2}{4}+\left(\frac{1}{\mathcal{A}+1}\right)^2 q^2+pQ\cos(\theta_p)+2\frac{1}{\mathcal{A}+1}pq\cos\left(\theta_q-\theta_p\right)+\frac{1}{\mathcal{A}+1}Qq\cos\left(\theta_q\right)\right)^{1/2}$
- $\left|\vec{p}-\frac{\vec{Q}}{2}-\frac{\mathcal{A}}{\mathcal{A}+1}\vec{q}\right| = \left(p^2+\frac{Q^2}{4}+\left(\frac{\mathcal{A}}{\mathcal{A}+1}\right)^2 q^2-pQ\cos(\theta_p)-2\frac{\mathcal{A}}{\mathcal{A}+1}pq\cos\left(\theta_q-\theta_p\right)+\frac{\mathcal{A}}{\mathcal{A}+1}Qq\cos\left(\theta_q\right)\right)^{1/2}$
- $\left|\vec{p}-\frac{\vec{Q}}{2}+\frac{1}{\mathcal{A}+1}\vec{q}\right| = \left(p^2+\frac{Q^2}{4}+\left(\frac{1}{\mathcal{A}+1}\right)^2 q^2-pQ\cos(\theta_p)+2\frac{1}{\mathcal{A}+1}pq\cos\left(\theta_q-\theta_p\right)-\frac{1}{\mathcal{A}+1}Qq\cos\left(\theta_q\right)\right)^{1/2}$
- $H_0(\vec{p}+\frac{\vec{Q}}{2},\vec{q}) = \frac{1}{2m_{jk}}\left(p^2+\frac{\vec{Q}}{2}+pQ\cos(\theta_p)\right)+\frac{1}{2m_{jk,i}}q^2$
- $H_0(\vec{p}-\frac{\vec{Q}}{2},\vec{q}) = \frac{1}{2m_{jk}}\left(p^2+\frac{\vec{Q}}{2}-pQ\cos(\theta_p)\right)+\frac{1}{2m_{jk,i}}q^2$

## D.2 The shifted momenta between particles A and C

The shifted momenta and the Hamiltonian can be written as

- $\left|\vec{p}+\frac{\vec{Q}}{2}-\frac{1}{\mathcal{B}+1}\vec{q}\right| = \left(p^2+\frac{Q^2}{4}+\left(\frac{1}{\mathcal{B}+1}\right)^2 q^2+pQ\cos(\theta_p)-2\frac{1}{\mathcal{B}+1}pq\cos\left(\theta_q-\theta_p\right)-\frac{1}{\mathcal{B}+1}Qq\cos\left(\theta_q\right)\right)^{1/2}$
- $\left|\vec{p}+\frac{\vec{Q}}{2}+\frac{\mathcal{B}}{\mathcal{B}+1}\vec{q}\right| = \left(p^2+\frac{Q^2}{4}+\left(\frac{\mathcal{B}}{\mathcal{B}+1}\right)^2 q^2+pQ\cos(\theta_p)+2\frac{\mathcal{B}}{\mathcal{B}+1}pq\cos\left(\theta_q-\theta_p\right)+\frac{\mathcal{B}}{\mathcal{B}+1}Qq\cos\left(\theta_q\right)\right)^{1/2}$
- $\left|\vec{p}-\frac{\vec{Q}}{2}-\frac{1}{\mathcal{B}+1}\vec{q}\right| = \left(p^2+\frac{Q^2}{4}+\left(\frac{1}{\mathcal{B}+1}\right)^2 q^2-pQ\cos(\theta_p)-2\frac{1}{\mathcal{B}+1}pq\cos\left(\theta_q-\theta_p\right)+\frac{1}{\mathcal{B}+1}Qq\cos\left(\theta_q\right)\right)^{1/2}$
- $\left|\vec{p}-\frac{\vec{Q}}{2}+\frac{\mathcal{B}}{\mathcal{B}+1}\vec{q}\right| = \left(p^2+\frac{Q^2}{4}+\left(\frac{\mathcal{B}}{\mathcal{B}+1}\right)^2 q^2-pQ\cos(\theta_p)+2\frac{\mathcal{B}}{\mathcal{B}+1}pq\cos\left(\theta_q-\theta_p\right)-\frac{\mathcal{B}}{\mathcal{B}+1}Qq\cos\left(\theta_q\right)\right)^{1/2}$

- $H_0(\vec{p}+\frac{\vec{Q}}{2},\vec{q}) = \frac{1}{2m_{ik}}\left(p^2+\frac{\vec{Q}}{2}+pQ\cos(\theta_p)\right)+\frac{1}{2m_{ik,j}}q^2$
- $H_0(\vec{p}-\frac{\vec{Q}}{2},\vec{q}) = \frac{1}{2m_{ik}}\left(p^2+\frac{\vec{Q}}{2}-pQ\cos(\theta_p)\right)+\frac{1}{2m_{ik,j}}q^2$

## D.3 The shifted momenta between particles A and B

The shifted momenta and the Hamiltonian can be written as

- $\left|\vec{p}+\frac{\vec{Q}}{2}-\frac{\mathcal{B}}{\mathcal{A}+\mathcal{B}}\vec{q}\right| = \left(p^2+\frac{Q^2}{4}+\left(\frac{\mathcal{B}}{\mathcal{A}+\mathcal{B}}\right)^2q^2+pQ\cos(\theta_p)-2\frac{\mathcal{B}}{\mathcal{A}+\mathcal{B}}pq\cos\left(\theta_q-\theta_p\right)-\frac{\mathcal{B}}{\mathcal{A}+\mathcal{B}}Qq\cos\left(\theta_q\right)\right)^{1/2}$
- $\left|\vec{p}+\frac{\vec{Q}}{2}+\frac{\mathcal{A}}{\mathcal{A}+\mathcal{B}}\vec{q}\right| = \left(p^2+\frac{Q^2}{4}+\left(\frac{\mathcal{A}}{\mathcal{A}+\mathcal{B}}\right)^2q^2+pQ\cos(\theta_p)+2\frac{\mathcal{A}}{\mathcal{A}+\mathcal{B}}pq\cos\left(\theta_q-\theta_p\right)+\frac{\mathcal{A}}{\mathcal{A}+\mathcal{B}}Qq\cos\left(\theta_q\right)\right)^{1/2}$
- $\left|\vec{p}-\frac{\vec{Q}}{2}-\frac{\mathcal{B}}{\mathcal{A}+\mathcal{B}}\vec{q}\right| = \left(p^2+\frac{Q^2}{4}+\left(\frac{\mathcal{B}}{\mathcal{A}+\mathcal{B}}\right)^2q^2-pQ\cos(\theta_p)-2\frac{\mathcal{B}}{\mathcal{A}+\mathcal{B}}pq\cos\left(\theta_q-\theta_p\right)+\frac{\mathcal{B}}{\mathcal{A}+\mathcal{B}}Qq\cos\left(\theta_q\right)\right)^{1/2}$
- $\left|\vec{p}-\frac{\vec{Q}}{2}+\frac{\mathcal{A}}{\mathcal{A}+\mathcal{B}}\vec{q}\right| = \left(p^2+\frac{Q^2}{4}+\left(\frac{\mathcal{A}}{\mathcal{A}+\mathcal{B}}\right)^2q^2-pQ\cos(\theta_p)+2\frac{\mathcal{A}}{\mathcal{A}+\mathcal{B}}pq\cos\left(\theta_q-\theta_p\right)-\frac{\mathcal{A}}{\mathcal{A}+\mathcal{B}}Qq\cos\left(\theta_q\right)\right)^{1/2}$
- $H_0(\vec{p}+\frac{\vec{Q}}{2},\vec{q}) = \frac{1}{2m_{ij}}\left(p^2+\frac{\vec{Q}}{2}+pQ\cos(\theta_p)\right)+\frac{1}{2m_{ij,k}}q^2$
- $H_0(\vec{p}-\frac{\vec{Q}}{2},\vec{q}) = \frac{1}{2m_{ij}}\left(p^2+\frac{\vec{Q}}{2}-pQ\cos(\theta_p)\right)+\frac{1}{2m_{ij,k}}q^2$

# BIBLIOGRAPHY


[1] C. J. Pethick and H. Smith, Bose-Einstein Condensation in Dilute Gases (Cambridge University Press) Chap. 5 (2008).

[2] G. Modugno, F. Ferlaino, R. Heidemann, G. Roati and M. Inguscio, Phys. Rev. A **68**, 011601 (2003).

[3] K. Günter, T. Stöferle, H. Moritz, M. Köhl and T. Esslinger, Phys. Rev. Lett. **95**, 230401 (2005).

[4] F. Werner and Y. Castin, Phys. Rev. A **86**, 053633 (2012).

[5] F. F. Bellotti and M. T. Yamashita, Few-Body Syst. **56**, 905 (2015).

[6] M. Kunitski et al., Science **348**, 551 (2015).

[7] W. Cencek et al., J. Chem. Phys. **136**, 224303 (2012).

[8] E. A. Kolganova, A. K. Motovilov and W. Sandhas, Few-Body Syst. **51**, 249 (2011).

[9] A. S. Jensen, K. Riisager, D. V. Fedorov and E. Garrido, Rev. Mod. Phys. **76**, 215 (2004).

[10] E. Braaten and H. W. Hammer, Phys. Rep. **428**, 259 (2006).

[11] T. Frederico, L. Tomio, A. Delfino, M. R. Hadizadeh and M. T. Yamashita, Few-Body Syst. **51**, 87 (2011).

[12] G. V. Skornyakov and K. A. Ter-Martirosyan, Sov. Phys. JETP **4**, 648 (1957).

[13] V. Efimov, Phys. Lett. B **33**, 563 (1970); V. Efimov, , Nucl. Phys. A **362**, 45 (1981).

[14] E. Nielsen, D. V. Fedorov, A. S. Jensen and E. Garrido, Phys. Rep. **347**, 373 (2001).

[15] L. W. Bruch and J. A. Tjon, Phys. Rev. A **19**, 425 (1979).

[16] S. K. Adhikari, Am. J. Phys. **54**, 362 (1986).

[17] S. K. Adhikari, A. Delfino, T. Frederico and L. Tomio, Phys. Rev. A **47**, 1093 (1993).

[18] F. F. Bellotti, T. Frederico, M. T. Yamashita, D. V. Fedorov, A. S. Jensen and N. T. Zinner, J. Phys. B **44**, 205302 (2011).

[19] F. F. Bellotti, T. Frederico, M. T. Yamashita, D. V. Fedorov, A. S. Jensen and N. T. Zinner, Phys. Rev. A **85**, 025601 (2012).

[20] F. F. Bellotti, T. Frederico, M. T. Yamashita, D. V. Fedorov, A. S. Jensen and N. T. Zinner, J. Phys. B **46**, 055301 (2013).

[21] N. N. Khuri, A. Martin and T.-T. Wu, Few-Body Syst. **31**, 83 (2002).

[22] J. Levinsen, P. Massignan and M. M. Parish, Phys. Rev. X **4**, 031020 (2014).

[23] M. T. Yamashita, R. S. Marques de Carvalho, L. Tomio and T. Frederico, Phys. Rev. A **68**, 012506 (2003).

[24] T. K. Lim and B. Shimer, Z. Phys. A **297**, 185 (1980).

[25] E. Nielsen, D.V. Fedorov, A.S. Jensen, and E. Garrido Phys.Rep.**347**, 373 (2001).

[26] L.D. Faddeev Soviet Phys. JETP **12** 1014 (1961)

[27] S. K. Adhikari et al. MODEL INDEPENDENCE OF SCATTERING OF 3 IDENTICAL BOSONS IN 2 DIMENSIONS. Physical Review A. College Pk: American Physical Soc, v. **47**, n. 2, p. 1093-1100, 1993.

[28] S. K. Adhikari. (1986) Quantum scattering in two dimensions. Am. J. Phys. **54**, 362.

[29] B. A. Lippmann, (1956), Phys. Rev. **102**, 264.

[30] L. L. Foldy, and W. Tobocman (1957), Phys. Rev. **105**, 1099.

[31] S. T. Epstein, (1957), Phys. Rev. **106**, 598.

[32] L.D. Faddeev, (1960), Zh. Eksp. i Teor. Fiz. **39**, 1459,[(1961), Soviet Phys. JETP **12**,1014];(1961), Dokl. Akad. Nauk SSSR **138**,565 [(1961), Soviet Phys.-Dokl. **6**, 384];(1962), Dokl. Akad. Nauk SSSR **145**,301 [(1963), Soviet Phys.-Dokl. **7**, 600];(1963), Mathematical Aspects of the Three-Body Problems in Quantum Scattering Theory (Steklov Math. Inst., Leningrad), (Engl. transl. D. Dave and Co., New York, 1965).

[33] S. Weinberg, (1964), Phys. Rev. **133**, B232.

[34] L. D. Faddeev, (1961), Soviet Phys. JETP **12**, 5.

[35] C. Lovelace, (1964), in Strong Interactions and High-Energy Physics, ed. R. G. Moorhouse (Oliver and Boyd, London); (1964), Phys. Rev. **135**, B1225.

[36] F. Riez, and B. Sz. Nagy (1955), Functional Analysis (Ungar, New York).

[37] L. V. Kantorovich, and G. P. Akilov (1964), Functional Analysis in Normed Spaces (Macmillan, New York).

[38] Charles J. Joachain. Quantum Collision Theory. North-Holland, (1983).

[39] M.T. Yamashita. Sistemas Fracamente Ligados de Três Corpos: Moléculas e Núcleos Exóticos Leves. PhD thesis, Universidade de São Paulo, 2004.

[40] F.F. Bellotti. Two- and three-dimensional few-body systems in the universal regime. PhD thesis, Department of Physics and Astronomy, Aarhus University, Denmark, 2014.

[41] T. Frederico, V. S. Timóteo & L. Tomio. Nucl. Phys. **A653**, 209 (1999).

[42] T. Frederico, A. Delfino & L. Tomio. Phys. Lett. **B481**, 143 (2000).

[43] T. Frederico. Hamiltonianas renormalizadas em mecânica quântica, tese de livre-docência, Universidade de São Paulo, 1998.

[44] A. N. Mitra. The Nuclear Three-Body Problem. Advances in Nuclear Physics, vol. **3**, 1969.

[45] E. W. Schmid and Horst Ziegelmann. The Quantum Mechanical Three-Body Problem. Pergamon Press, 1974.

[46] W. H. Press, Saul A. Teukolsky, William T. Vetterling and Brian P. Flannery. Numerical recipes 3rd edition: The art of scientific computing. Cambridge University Press, New York, NY, USA, 3 edition, 2007.

[47] Gerald Recktenwald. Numerical Methods With Matlab Implementation and Application. Prentice Hall, Upper Saddle River, New Jersey 07458, 2000.

[48] F. F. Bellotti, T. Frederico, M. T. Yamashita, D. V. Fedorov, A. S. Jensen and N. T. Zinner, J. Phys. B **44**, 205302 (2011).

[49] A. C. Fonseca, E. F. Redish and P. E. Shanley, Nucl. Phys. A **320**, 273 (1979).

[50] T. K. Lim and B. Shimer, Z. Phys. A **297**, 185 (1980)

[51] F. F. Bellotti, T. Frederico, M. T. Yamashita, D. V. Fedorov, A. S. Jensen and N. T. Zinner, J. Phys. B **46**, 055301 (2013).

[52] E. Nielsen, D. V. Fedorov, and A. S. Jensen Phys. Rev. A **56**, 3287 (1997).

[53] A. Messiah, Quantum Mechanics. North-Holland publishing company, amsterdam, vol (1), (1964)

[54] X. L. Yang, S. H. Guo, F. T. Chan, K. W. Wong, and W. Y. Ching Phys. Rev. A **43**, 1186 (1991).